Unraveling the Excitation Spectrum of the Nucleon
- the N* Program at Jefferson Lab

A.M. Sandorfi
Thomas Jefferson National Accelerator Facility, Virginia USA

- current quarks, constituent quarks & real world "dressings"
- the problem with the N* spectrum
  … and the hyperon solution – measurements of *everything*
- the CLAS g9/FROST and g14/HDice experiments
- *eg.* $\gamma p \rightarrow K^+\Lambda$ from what we know now,
  and what we can expect …

Excitation spectrum for A = 1

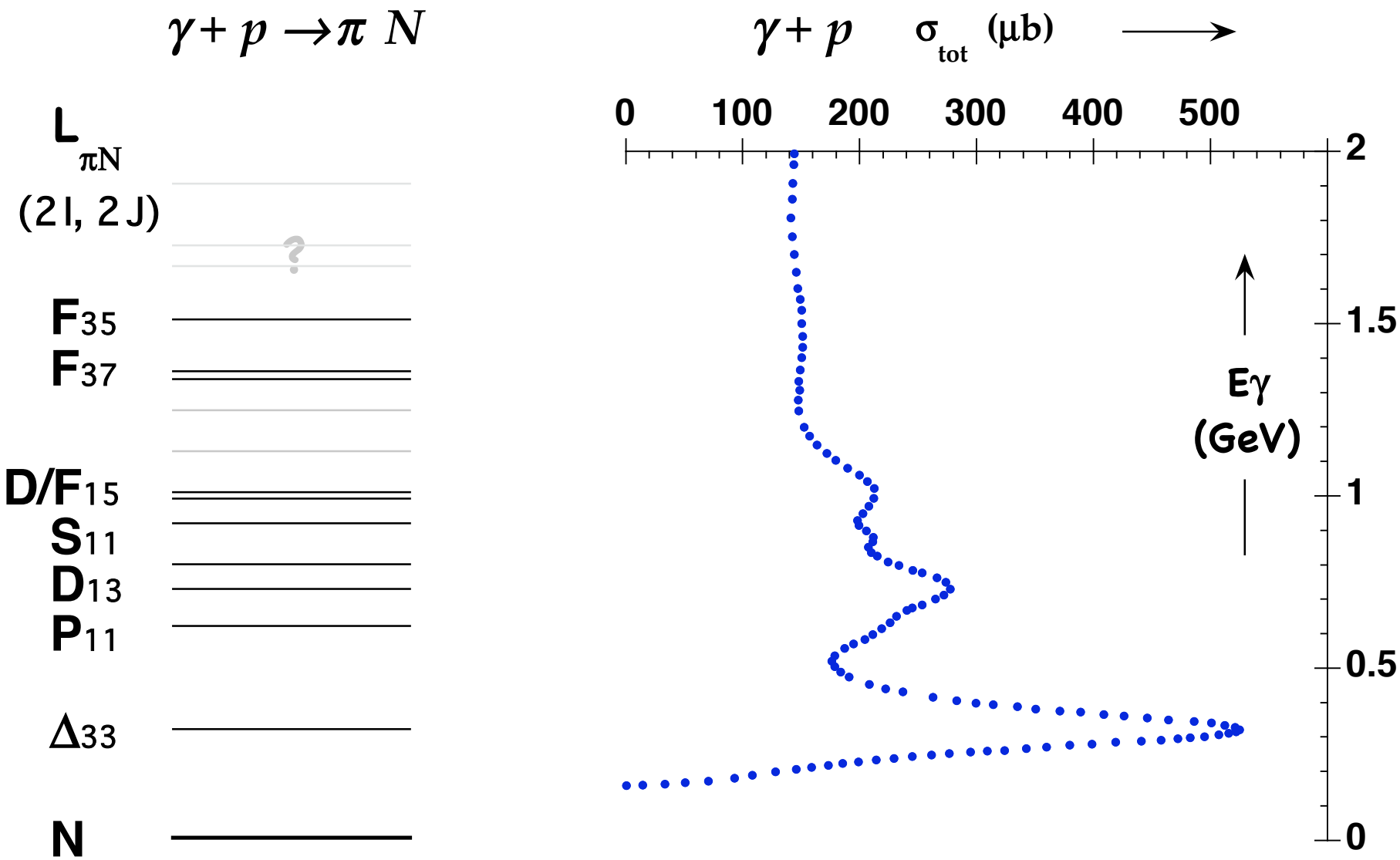

Spectrum & decay widths reflect the underlying nature of quark confinement and Chiral-Symmetry breaking in QCD

Connecting constituent quarks and current quarks in QCD

- viewed with Lattice-QCD and the Dyson-Schwinger eqn (ANL)

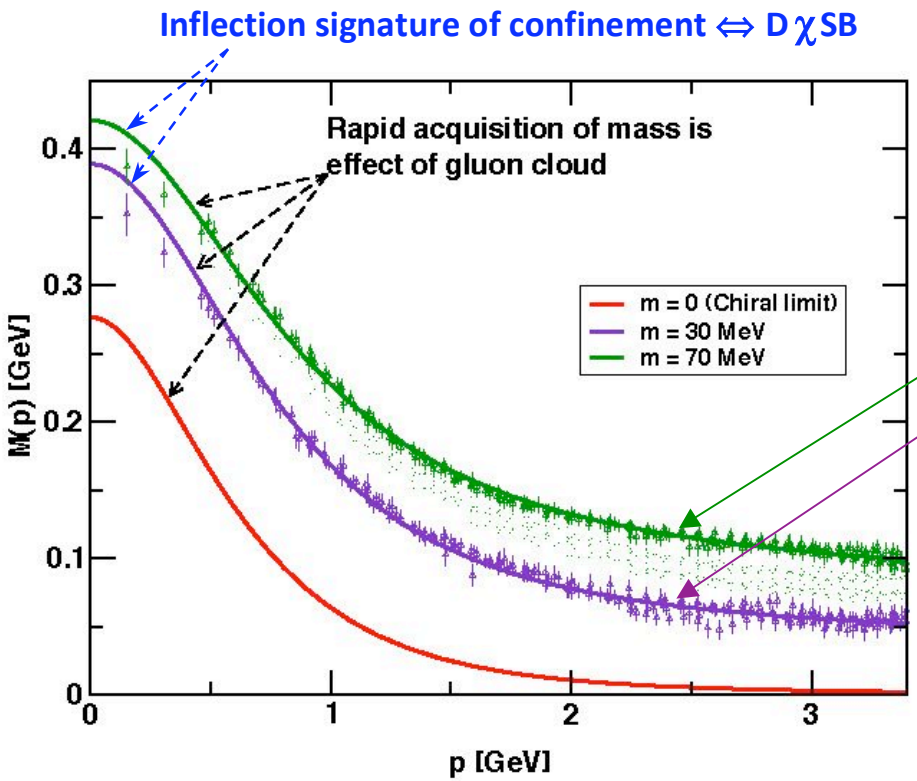

Craig Roberts

- quark propagators of DSE dressed with gluons (manifestation of dynamic Chiral-symmetry breaking)

+ LQCD (M_q = 70 MeV); —— DSE
+ LQCD (M_q = 30 MeV); —— DSE

—— DSE ($M_q \to 0$, Chiral-limit)

"constituent mass" appears at low p from a cloud of gluons that are dragged along as the quark propagates

- Connects the constituent mass of "QCD inspired" models ⇔ to the current quarks of the QCD Lagrangian

Excitation spectrum of the Nucleon

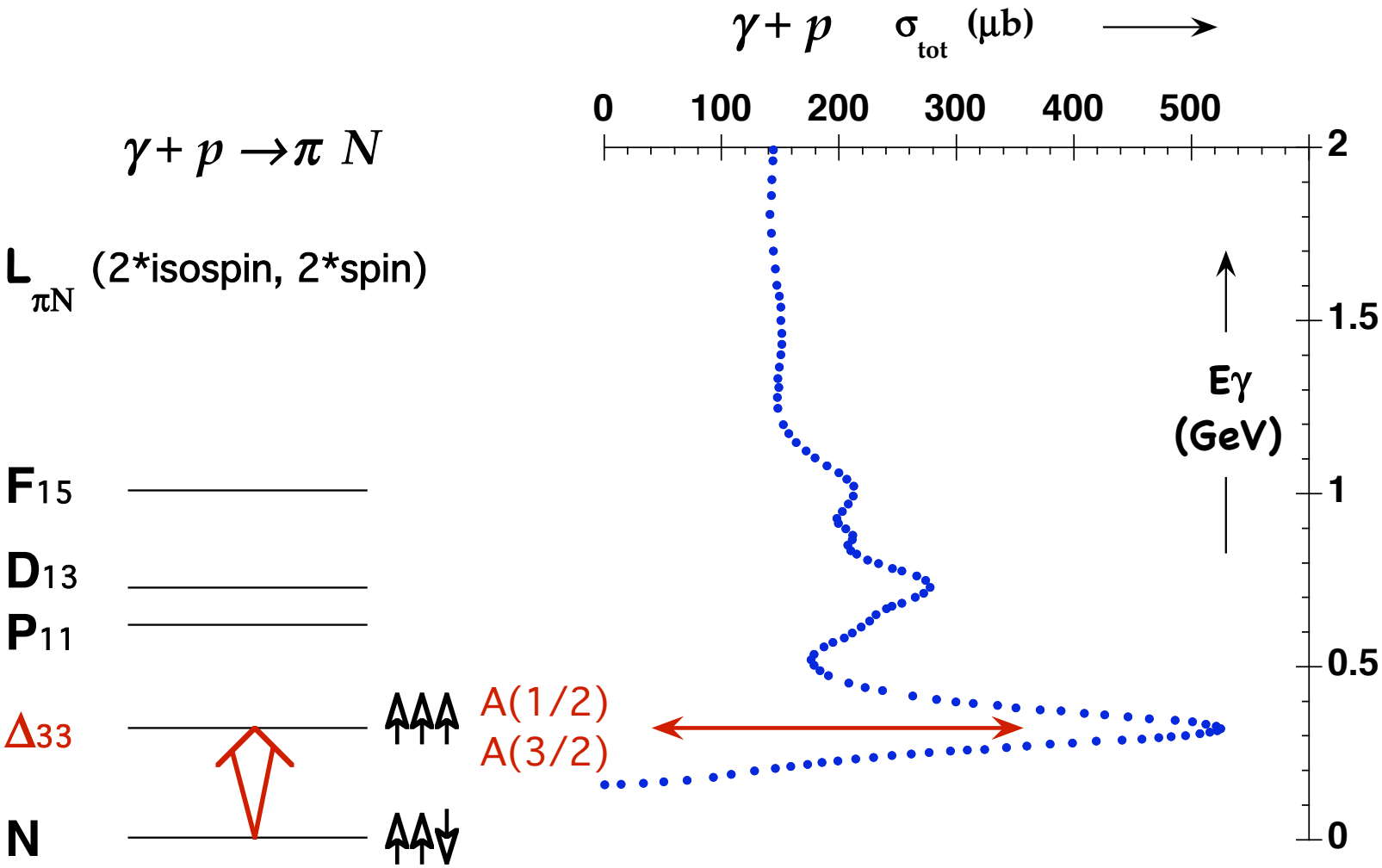

electron scattering

- one photon exchange
- vary Q^2 and W independently

$$e + p \Rightarrow \Delta_{33} + e'$$

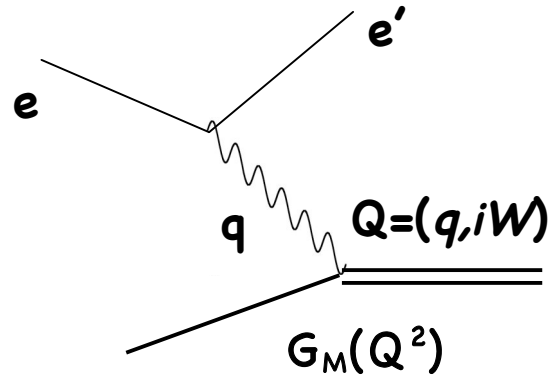

"dressed" interactions

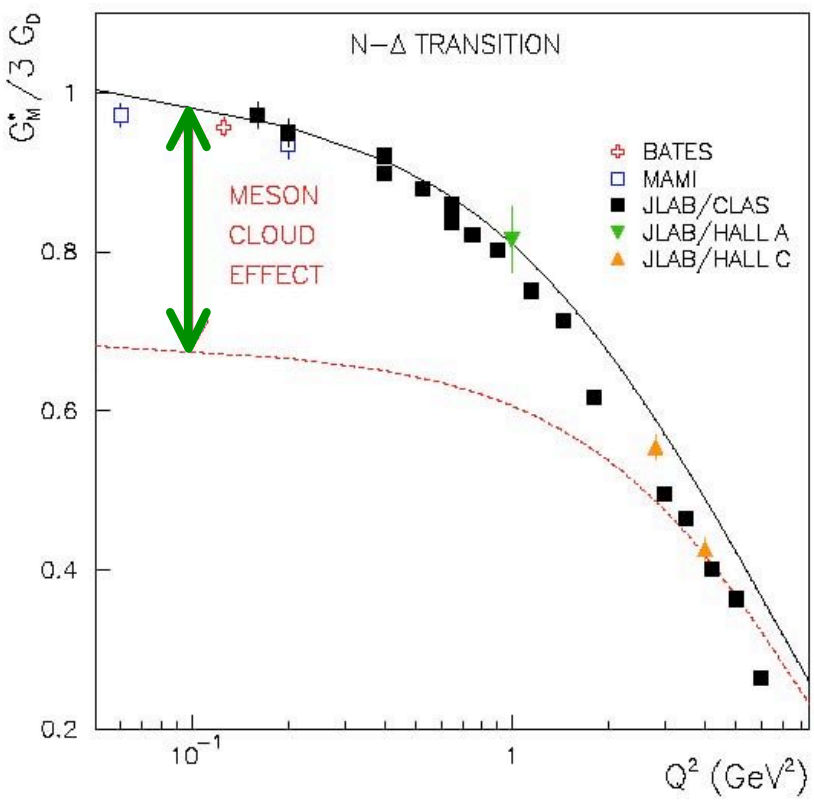

meson-cloud "dressing"
of the electromagnetic vertex

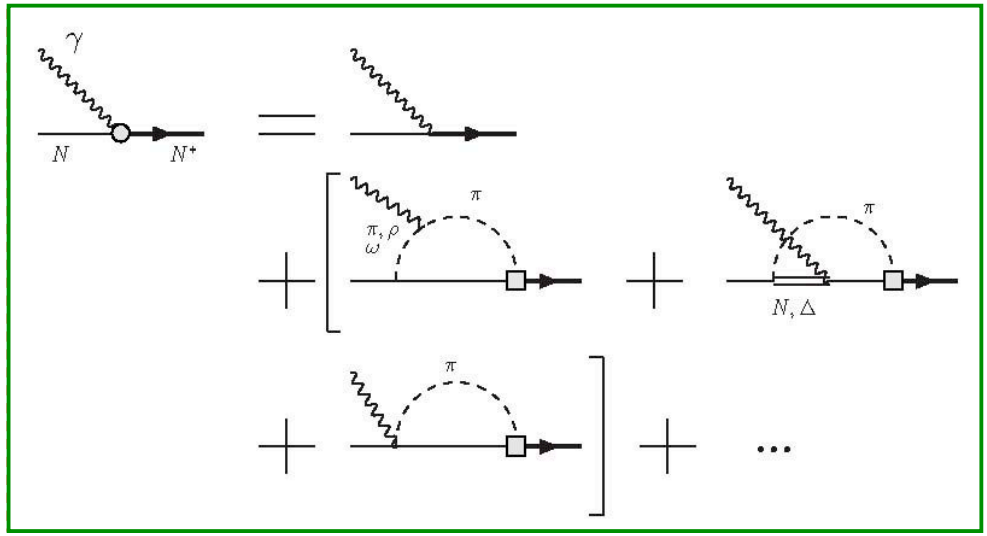

Harry Lee

"dressings" of the N* vertices

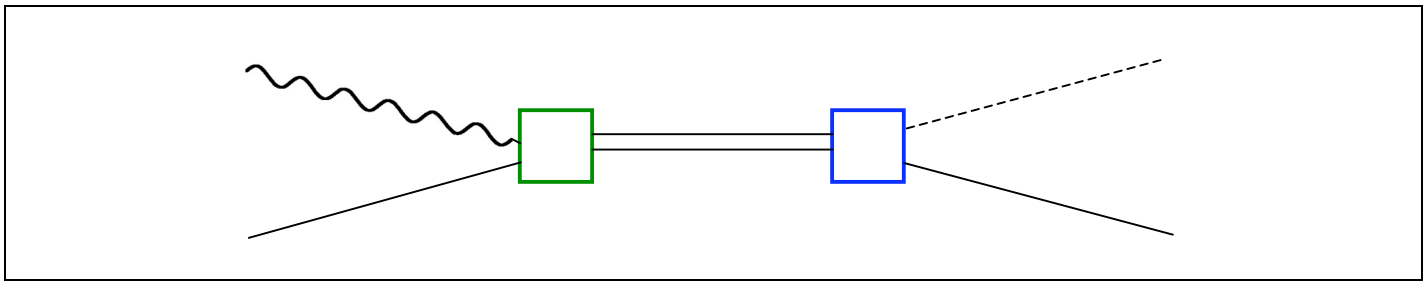

- "dressings" of the electro-magnetic vertex affect the dynamical properties and determine the Q^2 evolution of N* production, but <u>do not</u> affect spectral properties of the resonances.

- coupled-channel "dressings" of the strong vertex determine the spectral properties of the resonances, mass-pole positions, widths.

caveat: the detailed divisions between "dressings", "coupled-channel" effects and "core excitations" is model dependent, but on a course scale the divisions in physics remain fairly defined.

CC - baryon excited states coupled to meson-baryon channels

- a multi-channel, multi-resonance problem
- two particle channels: γN, πN, ηN, $K\Lambda$, $K\Sigma$, ωN
- three particle channels: $\pi\pi N$, with resonant components from $\pi\Delta$, ρN, σN
- must satisfy the Unitarity conditions connecting channels

eg. $\gamma p \rightarrow \pi N \rightarrow KY$
$\gamma p \rightarrow \pi\pi N \rightarrow KY$

- large **coupled-channel** effects !

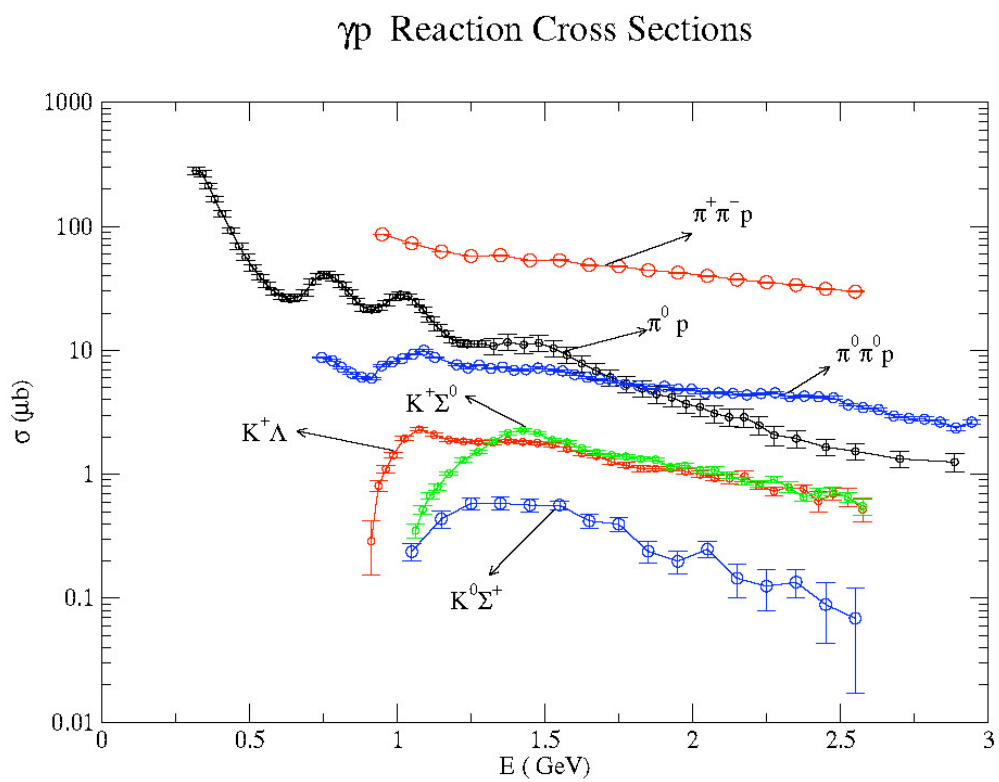

Harry Lee

Excitation spectrum of the Nucleon

$\gamma + p \rightarrow \pi N$

$L_{\pi N}$ (2*isospin, 2*spin)

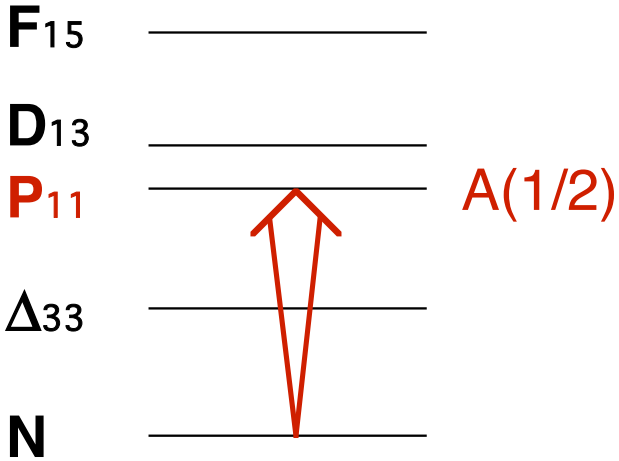

A(1/2)

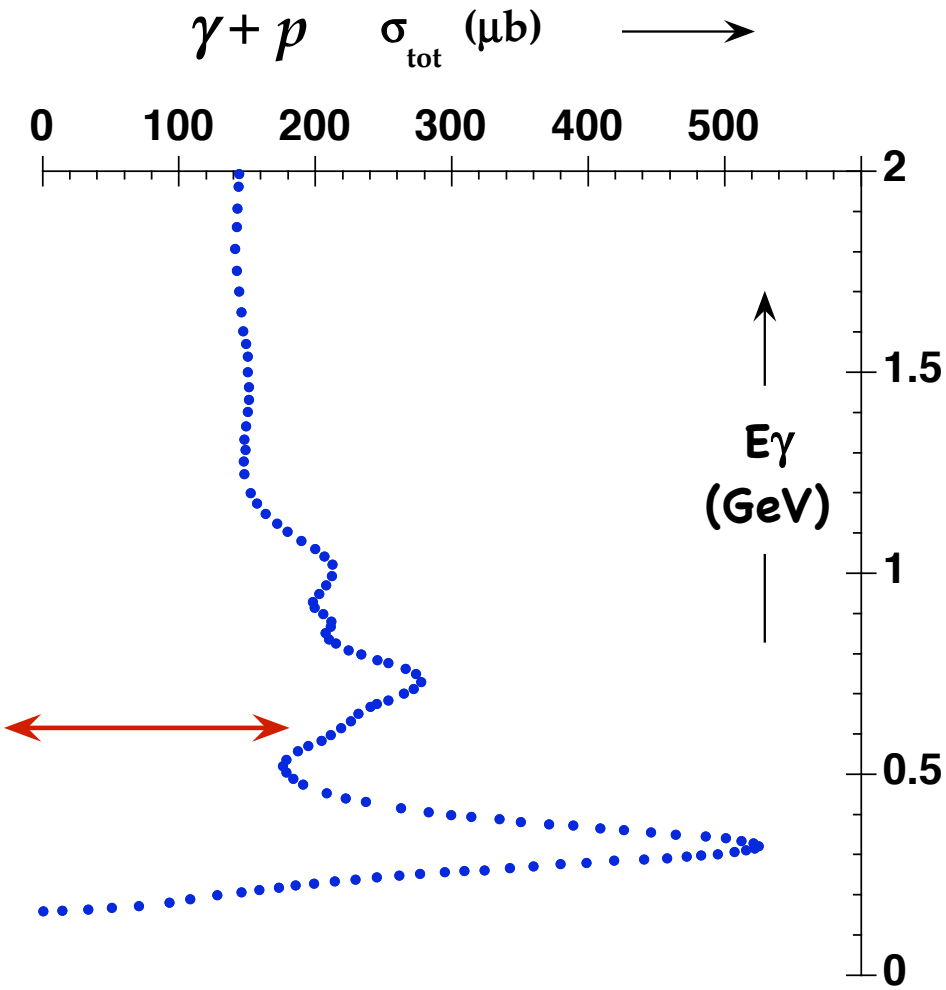

The puzzling P_{11}(W=1440) "*Roper*" resonance

- B. Feld and L.D. Roper, Siena Int. Conf. Elem. Part. Phy (1963)
- L.D. Roper, PRL 12, 340 (1964)
- PDG'08 $\Rightarrow$ W = 1420 -to- 1470 MeV
- recent PWA analysis suggests 2 poles - PRC 74, 045205 (06)
- decays into $N\pi$, $N\pi\pi$, $N\Delta$
- models of N* structure predict lowest P_{11} at much higher energy

  - qqq-g 3-quark-gluon hybrid ?
  - qqq 3-quark radial excitation ?

electron scattering
- one photon exchange
- vary Q^2 and W independently

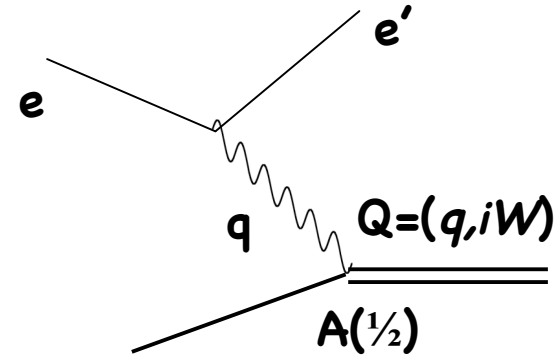

Amplitudes for P_{11} :

- transverse A(h=½)

CLAS data

● $\gamma\, p \rightarrow \pi\, N$

■ $\gamma\, p \rightarrow \pi\, \pi\, N$

PRC86 (12) 35203

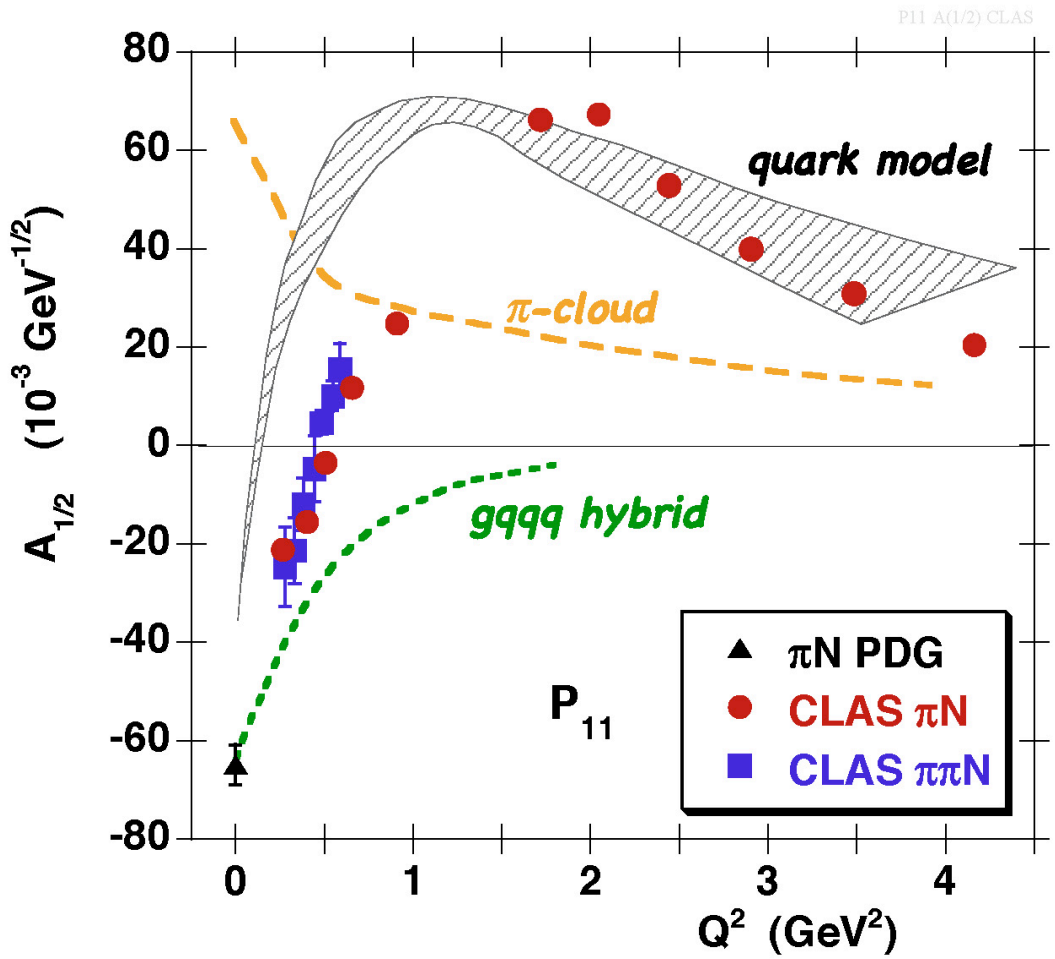

⇔ large π-cloud "dressing"

⇔ hybrid model (Li²-Burkert, PRD46) excluded

JLab-EBAC, PRL 104 (10) 042302

- **Dynamical coupled-channel model (πN, $\pi\pi N$, $\pi\Delta$, ηN, ρN, …)**
- **Resonance poles located numerically by analytic continuation**
- **1 channel ⇔ 1 pole; n channels ⇔ 2^n poles on 2^n Riemann sheets**

Evolution of a bare N^* into 3 P_{11} poles in EBAC-DCC model

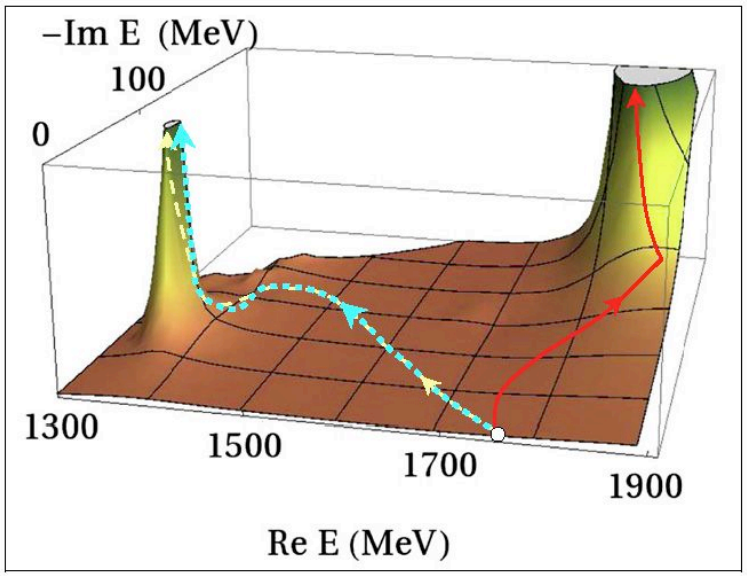

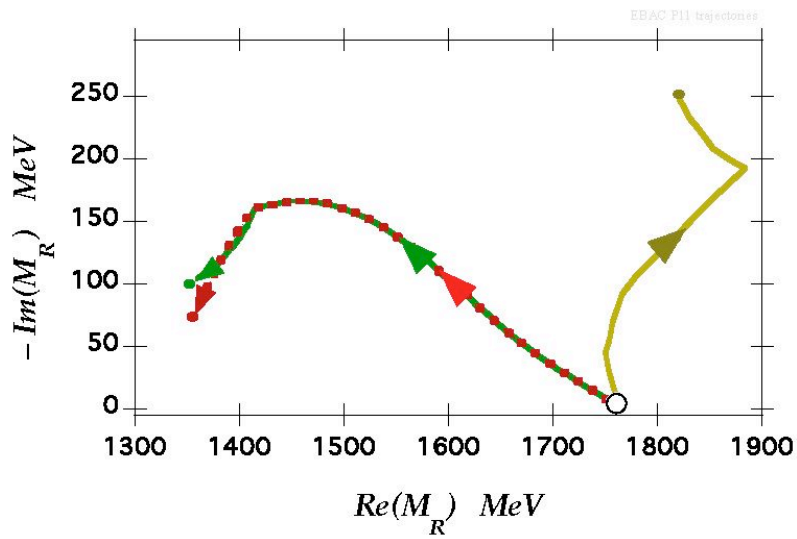

T.S.-H. Lee

$$T^R \propto \frac{1}{E - M_0^* - x\Sigma(E)}$$

EBAC(cc)-P11 trajectories_Im

The puzzling P_{11}(W=1440) "*Roper*" resonance

- B. Feld and L.D. Roper, Siena Int. Conf. Elem. Part. Phy (1963)
- L.D. Roper, PRL 12, 340 (1964)
- PDG'08 $\Rightarrow$ W = 1420 -to- 1470 MeV
- recent PWA analysis suggests 2 poles - PRC 74, 045205 (06)
- decays into $N\pi$, $N\pi\pi$, $N\Delta$
- models of N* structure predict lowest P_{11} at much higher energy

  - ~~qqq-g 3-quark-gluon hybrid ?~~ $\Leftrightarrow$ (e,e')
  - qqq 3-quark radial excitation

- 2 poles on each of the $N\pi$ and $N\pi\pi$ sheets
- through analytic continuation in DCC, P_{11} is seen as a quark core excitation that has to lie higher in energy in order to give the channel couplings (the "dressings" of the strong vertex) the space needed to bring the poles down to the observed energies

Unfolding and interpreting the N* spectrum

- LQCD and DSE ⇒ Chiral symmetry breaking of the QCD Lagrangian generates Constituent Q with effective masses & essential features captured in the CQM

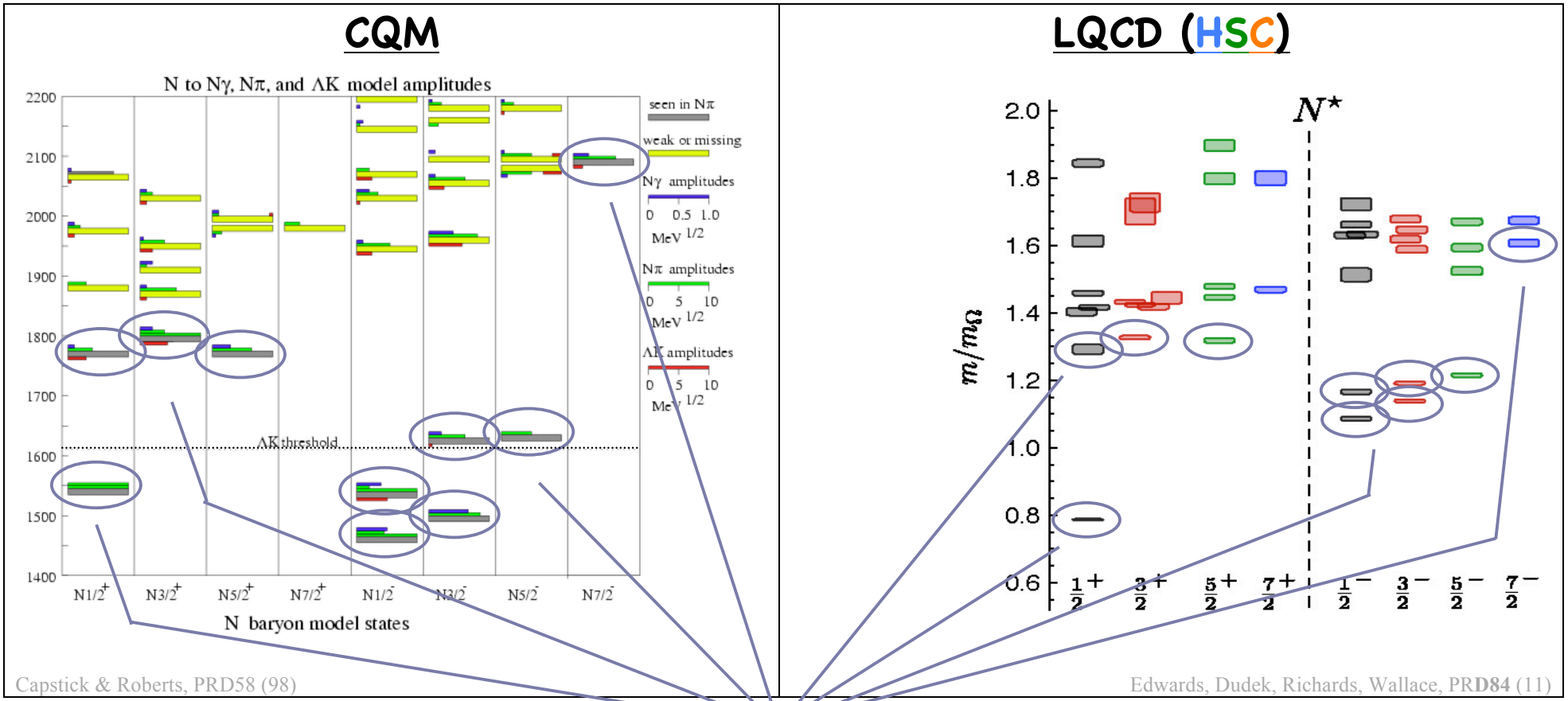

Capstick & Roberts, PRD58 (98)

Edwards, Dudek, Richards, Wallace, PRD84 (11)

- only lowest few in each band seen (in πN) with 4★ or 3★ status

Hyperons to the rescue ?

- higher levels predicted to have larger couplings to KΛ, KΣ, ππN, …

Comment regarding di-Quark excitations:

- 2 quarks quasibound in a color isotriplet; diquark+quark → color isosinglet

  Vintage diQuark models: [-eg. Anselmino *et al*, Rev. Mod. Phys. **65** (93)1199]
  - internal diquark excitations assumed frozen out
    (spin 0, isospin 0; no 20-plet configurations)

  ⇔ predicts approximately the same number of N* states seen in πN

DSE & LQCD:

- axial-vector color-triplet quark-quark correlations: ⇔ "di-Quarks"
  - <u>attractive</u> :

    $m[ud]_1 = m[uu]_1 = m[dd]_1 = 0.99 \pm .03$ GeV; $m[ud]_0 = 0.78 \pm .04$ GeV

  - <u>non-point-like</u>: *eg.* $r[ud]_1 = 0.8$ fm ~ pion radius [Few Body Sys 35(04); PRL97(06)]

Reality:

- diQuark configurations in the nucleon <u>very likely</u> (energetically favored)
- but they are not point-like ⇒ internal excitations highly likely
- diQuark correlations are already contained within the LQCD calculations

⇒ **diQuarks are not a solution to *missing* N* states**

Comment^2 regarding di-Quark excitations:

In fact, we probably have our 1st example:

- DSE: P_{11} Roper

  ⇔ a radial excitation of a diQuark coupled to the third quark

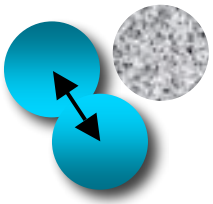

The problem:

N* structure lies encoded in the spectrum of the nucleon

⇔ **our challenge is to unravel the spectrum**

⇔ **search for resonance structure in the amplitudes**

- **ideal single isolated resonance**

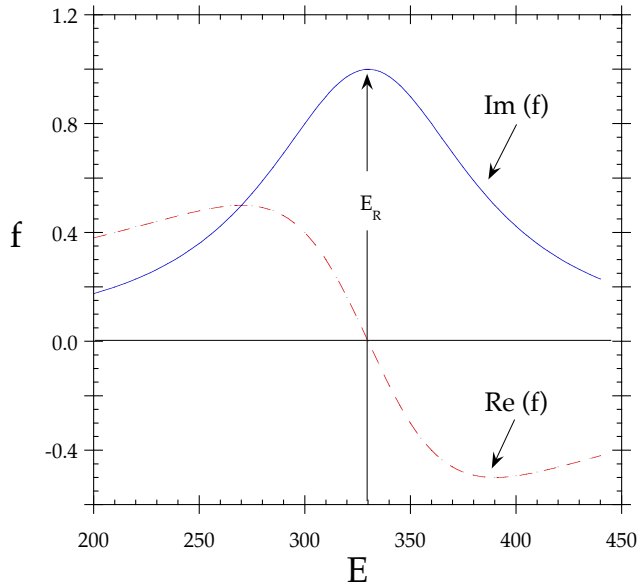

Argand plots:

- **counter-clockwise rotating amplitude**
  - characteristic resonance behavior

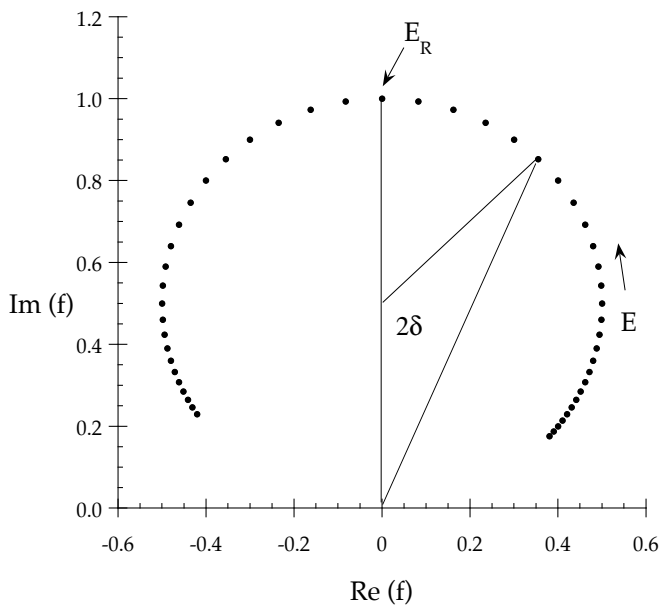

Argand - typical

The problem:

N* structure lies encoded in the spectrum of the nucleon

⇔ our challenge is to unravel the spectrum

Conventional approach:

- starting point: cross sections and a few polarization asymmetries
- parameterize the amplitude within a model;
  ⇒ fit model parameters to the data

A new plan:

- starting point: measure *everything !* (possible in hyperon channels)

⇒ experimental determination of meson production amplitudes

⇒ analytically continue the amplitude within a model to search for poles

- since electromagnetic interactions do not conserve isospin,
  this requires data on both the proton and the neutron

⇑	⇑
JLab-g9 (FROST)	JLab-g14 (HDice)

"Everything" in $J^\pi = 0^-$ meson photo-production

[SHKL, J Phys G38(11)053001]

$$d\sigma_{(B,T,R)} \equiv \sum \left| \textit{matrix elements} \right|^2 \times \left[\textit{polarization factors} \right]$$

$$\begin{aligned}
d\sigma_{(B,T,R)} = \tfrac{1}{2}\Big\{ & d\sigma_0 \cdot \left[1 - P_L^\gamma \cdot P_y^T \cdot P_{y'}^R \cos(2\phi_\gamma) \right] \\
& + \hat{\Sigma} \cdot \left[-P_L^\gamma \cos(2\phi_\gamma) + P_y^T \cdot P_{y'}^R \right] \\
& + \hat{T} \cdot \left[P_y^T - P_L^\gamma \cdot P_{y'}^R \cos(2\phi_\gamma) \right] \\
& + \hat{P} \cdot \left[P_{y'}^R - P_L^\gamma \cdot P_y^T \cos(2\phi_\gamma) \right] \\
& + \hat{E} \cdot \left[-P_c^\gamma \cdot P_z^T + P_L^\gamma \cdot P_x^T \cdot P_{y'}^R \sin(2\phi_\gamma) \right] \\
& + \hat{G} \cdot \left[P_L^\gamma \cdot P_z^T \sin(2\phi_\gamma) + P_c^\gamma \cdot P_x^T \cdot P_{y'}^R \right] \\
& + \hat{F} \cdot \left[P_c^\gamma \cdot P_x^T + P_L^\gamma \cdot P_z^T \cdot P_{y'}^R \sin(2\phi_\gamma) \right] \\
& + \hat{H} \cdot \left[P_L^\gamma \cdot P_x^T \sin(2\phi_\gamma) - P_c^\gamma \cdot P_z^T \cdot P_{y'}^R \right] \\
& + \hat{C}_{x'} \cdot \left[P_c^\gamma \cdot P_{x'}^R - P_L^\gamma \cdot P_y^T \cdot P_{z'}^R \sin(2\phi_\gamma) \right] \\
& + \hat{C}_{z'} \cdot \left[P_c^\gamma \cdot P_{z'}^R + P_L^\gamma \cdot P_y^T \cdot P_{x'}^R \sin(2\phi_\gamma) \right] \\
& + \hat{O}_{x'} \cdot \left[P_L^\gamma \cdot P_{x'}^R \sin(2\phi_\gamma) + P_c^\gamma \cdot P_y^T \cdot P_{z'}^R \right] \\
& + \hat{O}_{z'} \cdot \left[P_L^\gamma \cdot P_{z'}^R \sin(2\phi_\gamma) - P_c^\gamma \cdot P_y^T \cdot P_{x'}^R \right] \\
& + \hat{L}_{x'} \cdot \left[P_z^T \cdot P_{x'}^R + P_L^\gamma \cdot P_x^T \cdot P_{z'}^R \cos(2\phi_\gamma) \right] \\
& + \hat{L}_{z'} \cdot \left[P_z^T \cdot P_{z'}^R - P_L^\gamma \cdot P_x^T \cdot P_{x'}^R \cos(2\phi_\gamma) \right] \\
& + \hat{T}_{x'} \cdot \left[P_x^T \cdot P_{x'}^R - P_L^\gamma \cdot P_z^T \cdot P_{z'}^R \cos(2\phi_\gamma) \right] \\
& + \hat{T}_{z'} \cdot \left[P_x^T \cdot P_{z'}^R + P_L^\gamma \cdot P_z^T \cdot P_{x'}^R \cos(2\phi_\gamma) \right] \Big\}
\end{aligned}$$

Leading Pol dependence

Single Pol

beam+target

beam+recoil

target+recoil

Polarization observables in $J^{\pi} = 0^{-}$ meson photo-production : (SHKL, J Phys G**38** (11) 053001)

Photon beam		Target			Recoil			Target - Recoil								
					x'	y'	z'	x'	x'	x'	y'	y'	y'	z'	z'	z'
		x	y	z				x	y	z	x	y	z	x	y	z
unpolarized	σ_0		T			P		$T_{x'}$		$L_{x'}$		Σ		$T_{z'}$		$L_{z'}$
$P_L^{\gamma}\ \sin(2\phi_{\gamma})$		H		G	$O_{x'}$		$O_{z'}$		$C_{z'}$		E		F		$-C_{x'}$	
$P_L^{\gamma}\ \cos(2\phi_{\gamma})$	$-\Sigma$		$-P$			$-T$		$-L_{z'}$		$T_{z'}$		$-\sigma_0$		$L_{x'}$		$-T_{x'}$
circular P_c^{γ}		F		$-E$	$C_{x'}$		$C_{z'}$		$-O_{z'}$		G		$-H$		$O_{x'}$	

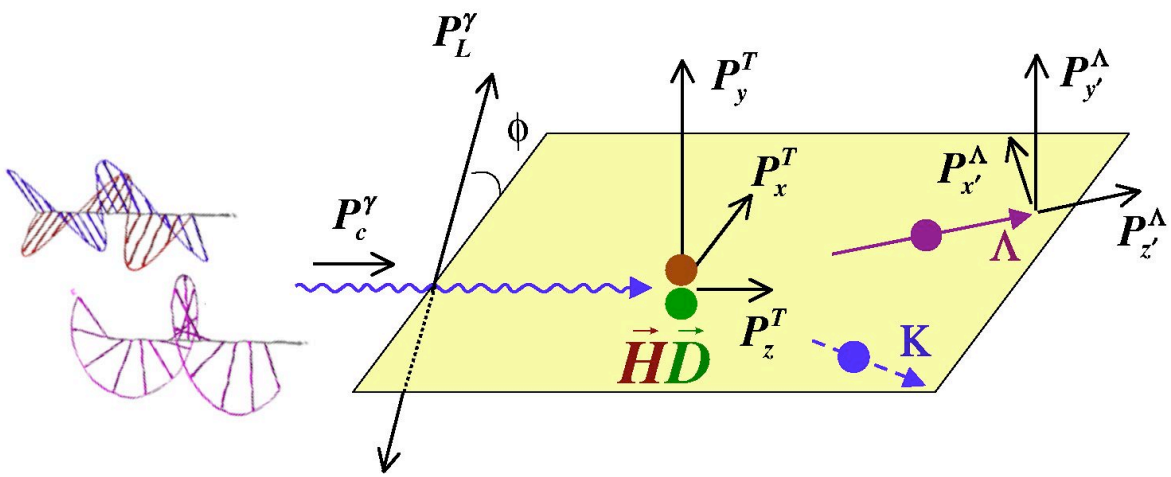

16 different observables, each appearing twice:

- ***single-pol observables can be measured from double-pol asy***
- ***double-pol observables can be measured from triple-pol asy***

Amplitudes and ambiguities:

- $\gamma + N \rightarrow (J^{\pi}=0^{-}) + N/\Lambda/\Sigma$

  spin states: $2 + 2 \rightarrow 0 + 2$ ⇒ 8 spin combinations
  ⇒ 4 unique (parity)

  ⇒ 4 complex amplitudes describe photo-production

  ⇒ 8 quantities to be determined

  ⇒ the 16 possible observables (matrix elements) are not independent

- uniqueness studies: Barker, Donnachie, Storrow, NP B95 (75) 347;
  Chiang, Tabakin, PR C55 (97) 2054

  ⇒ "mathematical solution" requires a set of 8 carefully chosen observables

  ⇒ avoiding ambiguities require asymmetries involving recoil polarization

$d\sigma\left(P^{\gamma}, P^{T}, P^{R}\right)$:

- Beam and Target polarizations are under experimental control

- **Recoil polarization - byproduct of entrance channel angular momentum (P^{γ}, P^{T}) and reaction physics ⇔ combinations of matrix elements**

⇒ **measurements of the recoil baryon polarization access combinations of spin-observables**

⇔ **a wealth of information !**

$d\sigma\left(P^{\gamma}, P^{T}, P^{R}\right)$:

- Beam and Target polarizations are under experimental control

- **Recoil polarization – byproduct of entrance channel angular momentum (P^{γ}, P^{T}) and reaction physics ⇔ combinations of matrix elements**

eg. 1 unpolarized beam and target:

$$\vec{P}^{R} = (0,\ P,\ 0)$$

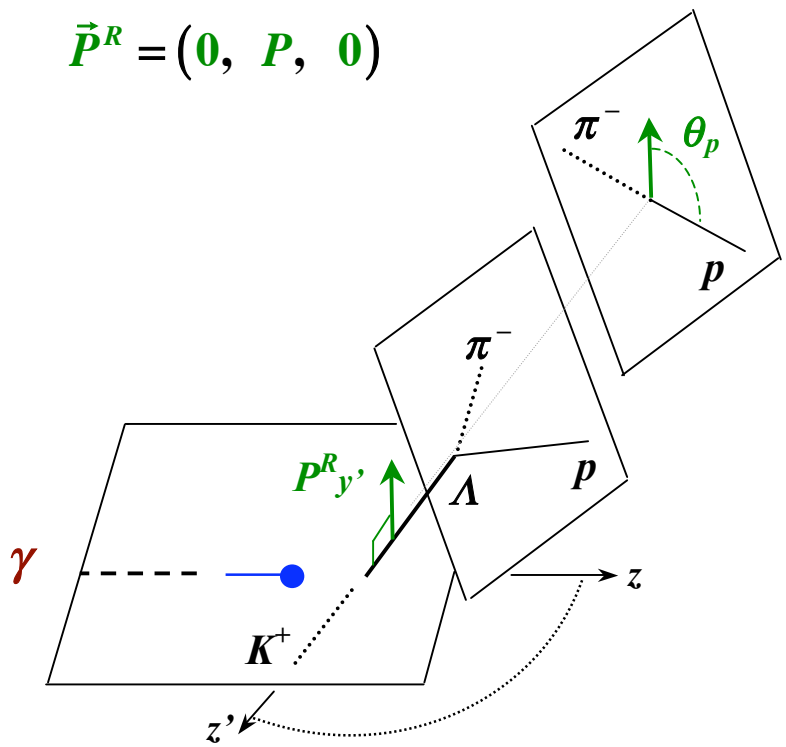

- **weak decay $\Lambda \rightarrow \pi^- p$**

- **angular distribution in Λ rest frame**

$$W(\theta_p) = \tfrac{1}{2}\left(1 + \alpha\left|\vec{P}_{\Lambda}\right|\cos(\theta_p)\right)$$

$$\Rightarrow\ P^{R}_{\Lambda} = \frac{2}{\alpha}\cdot\frac{N_{up} - N_{down}}{N_{up} + N_{down}}$$

α = 0.642 ± 0.013

eg. circularly polarized beam and longitudinally polarized target:

$$\vec{P}^R = \left(\frac{P_c^\gamma C_{x'} + P_z^T L_{x'}}{1 - P_c^\gamma P_z^T E}, \quad \frac{P - P_c^\gamma P_z^T H}{1 - P_c^\gamma P_z^T E}, \quad \frac{P_c^\gamma C_{z'} + P_z^T L_{z'}}{1 - P_c^\gamma P_z^T E} \right)$$

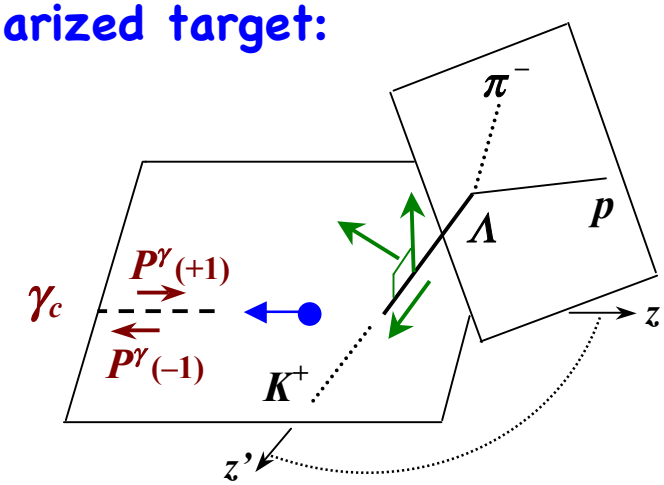

eg. circularly polarized beam and longitudinally polarized target:

$$\vec{P}^R = \left(\frac{P_c^\gamma C_{x'} + P_z^T L_{x'}}{1 - P_c^\gamma P_z^T E}, \quad \frac{P - P_c^\gamma P_z^T H}{1 - P_c^\gamma P_z^T E}, \quad \frac{P_c^\gamma C_{z'} + P_z^T L_{z'}}{1 - P_c^\gamma P_z^T E} \right)$$

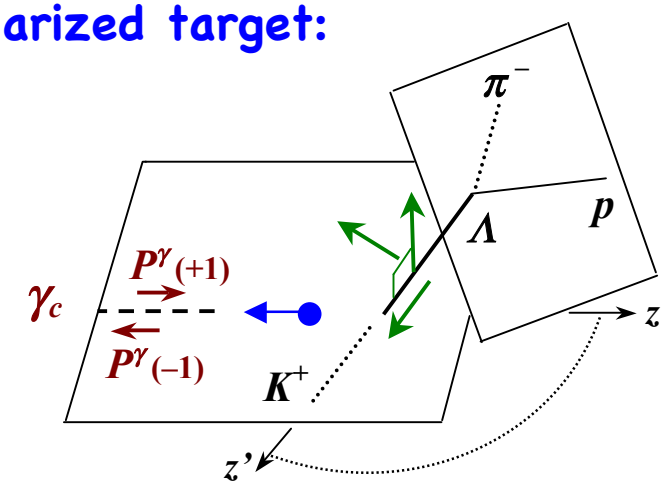

- sum final states (ignore recoil) : $\Rightarrow$ $d\sigma_0$ and E $\Leftrightarrow$ P^R denominator

eg. circularly polarized beam and longitudinally polarized target:

$$\vec{P}^R = \left(\frac{P_c^\gamma C_{x'} + P_z^T L_{x'}}{1 - P_c^\gamma P_z^T E}, \quad \frac{P - P_c^\gamma P_z^T H}{1 - P_c^\gamma P_z^T E}, \quad \frac{P_c^\gamma C_{z'} + P_z^T L_{z'}}{1 - P_c^\gamma P_z^T E} \right)$$

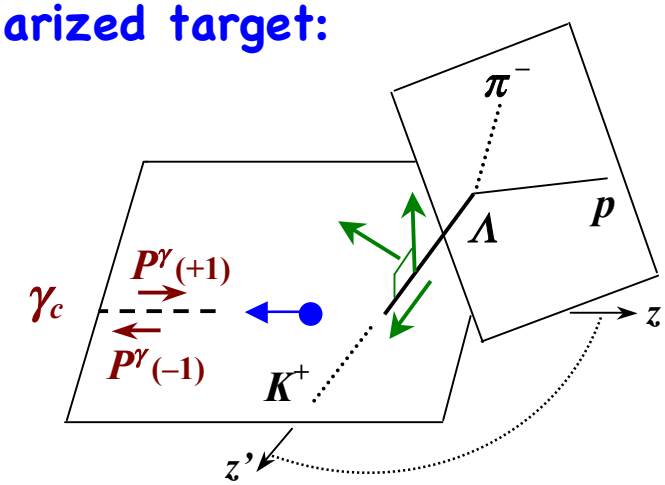

- sum final states (ignore recoil) : $\Rightarrow$ $d\sigma_0$ and E $\Leftrightarrow$ P^R denominator
- average initial target pol states ($\pm P_z^T$) : $\vec{P}^R \Rightarrow C_{x'}, P, C_{z'}$

eg. circularly polarized beam and longitudinally polarized target:

$$\vec{P}^R = \left(\frac{P_c^\gamma C_{x'} + P_z^T L_{x'}}{1 - P_c^\gamma P_z^T E}, \quad \frac{P - P_c^\gamma P_z^T H}{1 - P_c^\gamma P_z^T E}, \quad \frac{P_c^\gamma C_{z'} + P_z^T L_{z'}}{1 - P_c^\gamma P_z^T E} \right)$$

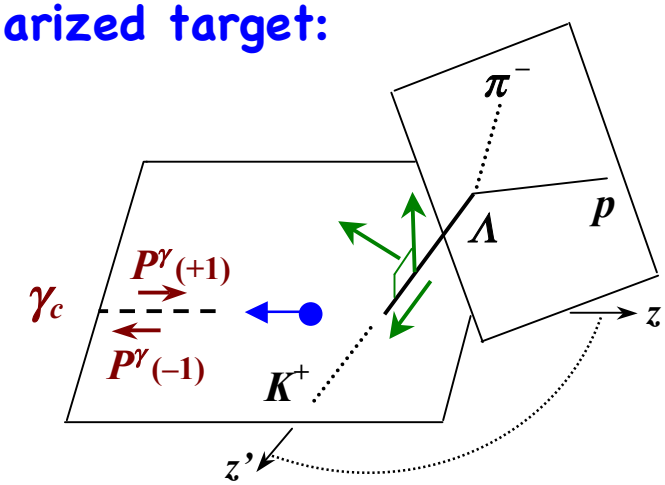

- sum final states (ignore recoil) : $\Rightarrow$ $d\sigma_0$ and E $\Leftrightarrow$ P^R denominator
- average initial target pol states ($\pm P_z^T$) : $\vec{P}^R \Rightarrow C_{x'}, P, C_{z'}$
- **average initial beam pol states ($P_c^\gamma(h=\pm 1)$) : $P_{x'}^R, P_{z'}^R \Rightarrow L_{x'}, L_{z'}$**

eg. circularly polarized beam and longitudinally polarized target:

$$\vec{P}^R = \left(\frac{P_c^\gamma C_{x'} + P_z^T L_{x'}}{1 - P_c^\gamma P_z^T E}, \quad \frac{P - P_c^\gamma P_z^T H}{1 - P_c^\gamma P_z^T E}, \quad \frac{P_c^\gamma C_{z'} + P_z^T L_{z'}}{1 - P_c^\gamma P_z^T E} \right)$$

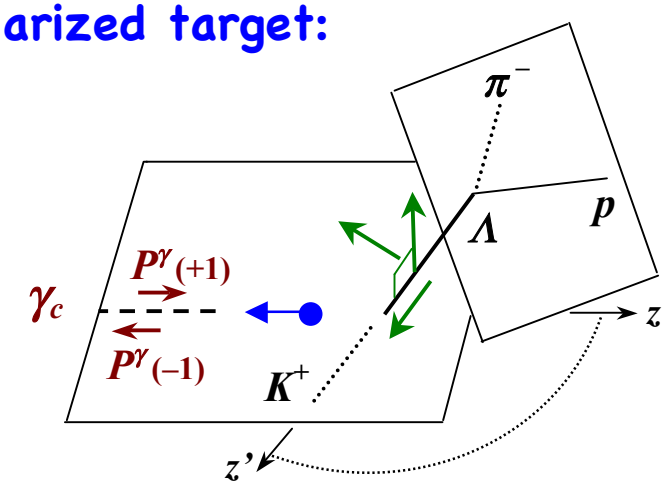

- sum final states (ignore recoil) : $\Rightarrow$ $d\sigma_0$ and E $\Leftrightarrow$ P^R denominator
- average initial target pol states ($\pm P_z^T$) : $\vec{P}^R \Rightarrow C_{x'}, P, C_{z'}$
- average initial beam pol states ($P_c^\gamma(h = \pm 1)$) : $P_{x'}^R, P_{z'}^R \Rightarrow L_{x'}, L_{z'}$
- **combining initial states** $P_c^\gamma \left(P_{+z}^T - P_{-z}^T \right)$ **:** $P_{y'}^R \Rightarrow H$

$$\Updownarrow$$

nominal "transverse target asy"

eg. circularly polarized beam and longitudinally polarized target:

$$\vec{P}^R = \left(\frac{P_c^\gamma C_{x'} + P_z^T L_{x'}}{1 - P_c^\gamma P_z^T E}, \quad \frac{P - P_c^\gamma P_z^T H}{1 - P_c^\gamma P_z^T E}, \quad \frac{P_c^\gamma C_{z'} + P_z^T L_{z'}}{1 - P_c^\gamma P_z^T E} \right)$$

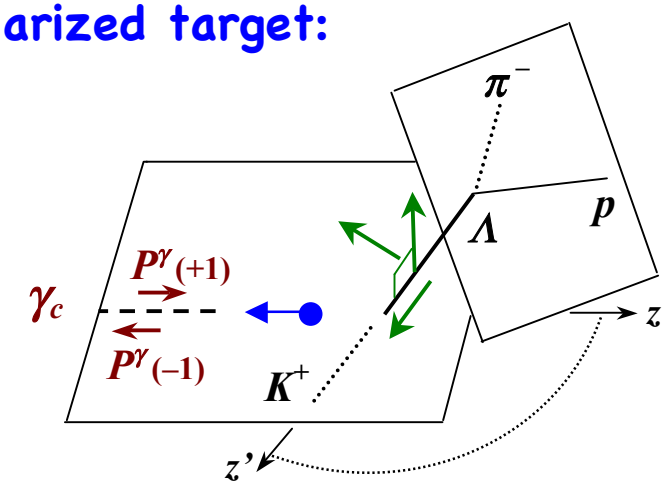

- sum final states (ignore recoil) : $\Rightarrow$ $d\sigma_0$ and E $\Leftrightarrow$ P^R denominator
- average initial target pol states ($\pm P_z^T$) : $\vec{P}^R \Rightarrow C_{x'}, P, C_{z'}$
- average initial beam pol states ($P_c^\gamma(h = \pm 1)$) : $P_{x'}^R, P_{z'}^R \Rightarrow L_{x'}, L_{z'}$
- combining initial states $P_c^\gamma \left(P_{+z}^T - P_{-z}^T \right)$: $P_{y'}^R \Rightarrow H$

$\Updownarrow$

nominal "transverse target asy"

(in all, 8 different observables)

Experimental options for recoil polarization:

- $\gamma N \rightarrow K \Lambda \Rightarrow K (\pi^- p)$, baryon decay peaked along Λ polarization, $\alpha_\Lambda = +0.64$
- $\gamma N \rightarrow K \Sigma^+ \Rightarrow K (\pi^0 p)$, baryon decay peaked along Σ polarization, $\alpha_\Sigma = -0.98$
- $\gamma N \rightarrow \pi N \Rightarrow \pi N'$, via asymmetry in 2nd scattering from ^{12}C, $\varepsilon \sim 0.01$ quite difficult, although cross sections are larger

The new plan:

- **collect data on all possible observables in $\sim 4\pi$ detectors**

  - with beam and target polarized, measurements of the recoil polarization allow the extraction of all 16 observables with a single target orientation

  [SHKL, J Phys G38 (11) 053001]

- **express the observables in terms of the amplitude**
- **fit the amplitude !**

Unraveling the Excitation Spectrum of the Nucleon
- the N* Program at Jefferson Lab

A.M. Sandorfi
Thomas Jefferson National Accelerator Facility, Virginia USA

- current quarks, constituent quarks & real world "dressings"
- the problem with the N* spectrum
  … and the hyperon solution – measurements of *everything*
- the CLAS g9/FROST and g14/HDice experiments
- *eg.* $\gamma p \rightarrow K^+\Lambda$ from what we know now,
  and what we can expect …

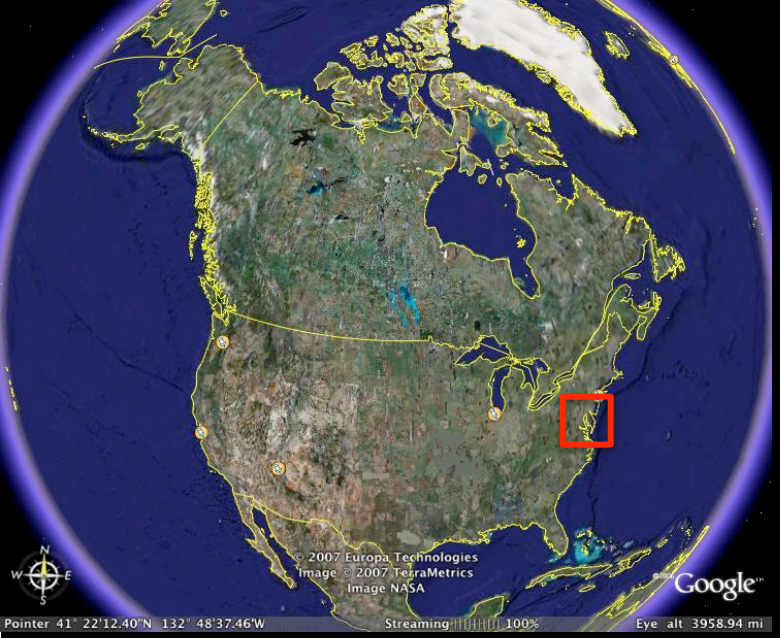

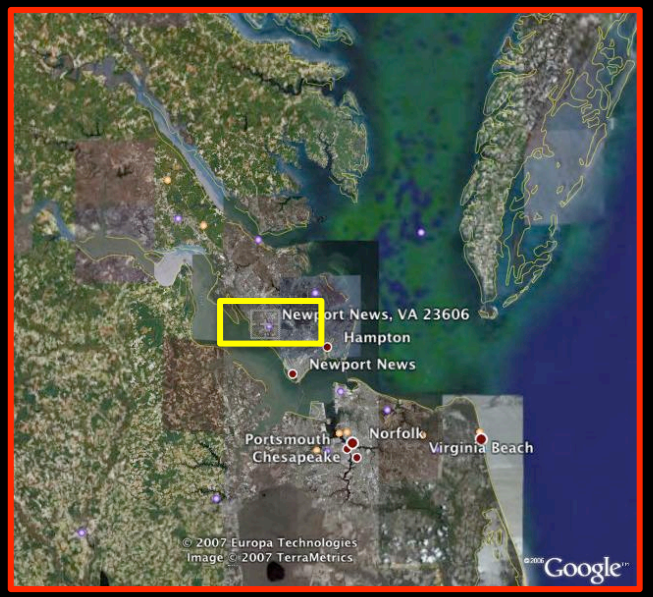

Jefferson Lab

The Hall B tool set: **C**EBAF **L**arge **A**cceptance **S**pectrometer

Torus magnet
6 superconducting coils

Electromagnetic calorimeters
Lead/scintillator, 1296 photomultipliers

polarized target + start counter

Drift chambers
argon/CO_2 gas, 35,000 cells

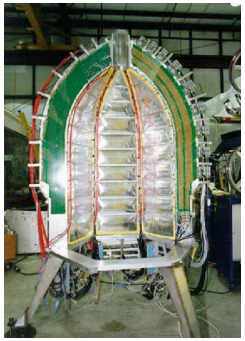

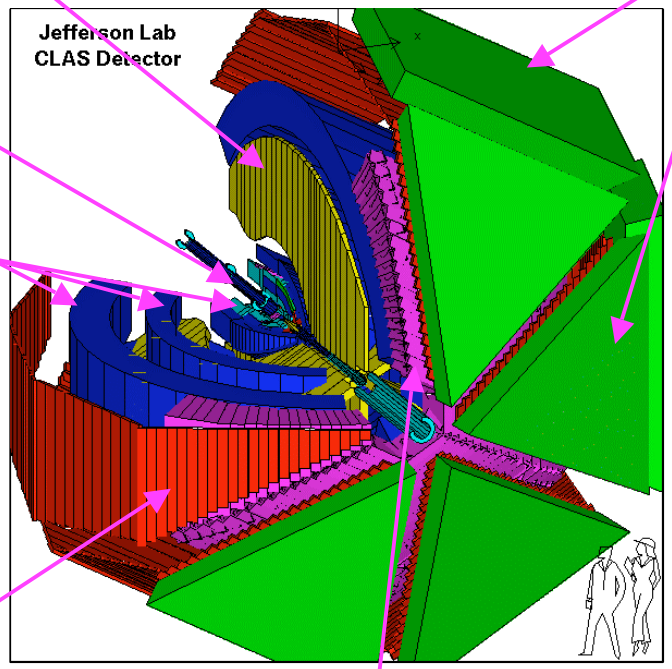

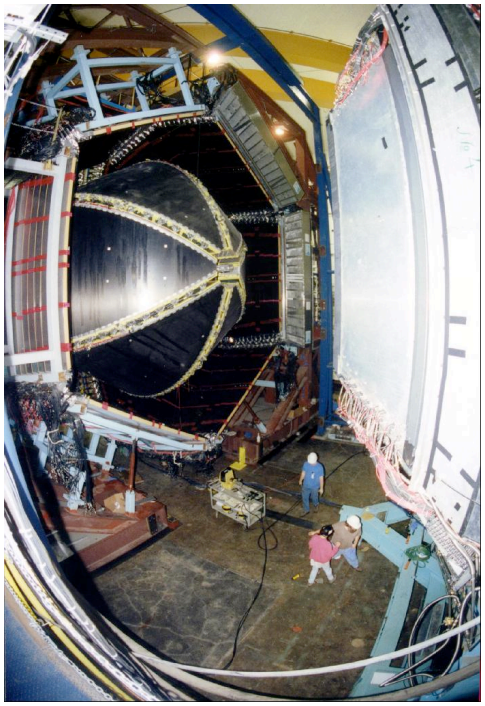

Time-of-flight counters
plastic scintillators, 684 photomultipliers

Gas Cherenkov counters
e/π separation, 256 PMTs

DAQ linit ~ 6kHz (~1.5TB/day)

Hall B Photon Tagger

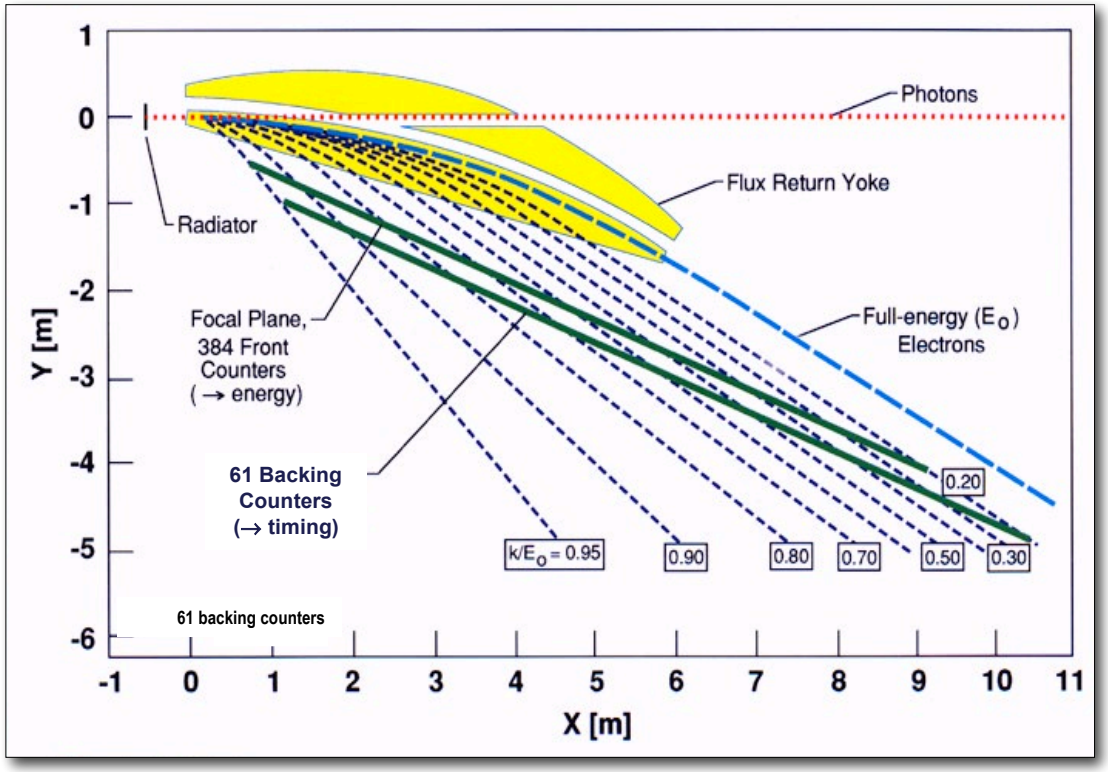

- bremsstrahlung photon tagger
- E_γ = 20-95% of E_0
- E_γ up to ~5.5 GeV

- Circularly polarized photons from longitudinally polarized electrons
- Linearly polarized photons from brem in oriented diamond crystals

Polarization observables in $\gamma p \rightarrow K^+\Lambda$ photo-production :

Photon beam		Target			Recoil			Target - Recoil								
					x'	y'	z'	x'	x'	x'	y'	y'	y'	z'	z'	z'
		x	y	z				x	y	z	x	y	z	x	y	z
unpolarized	σ_0		T			P		$T_{x'}$		$L_{x'}$		Σ		$T_{z'}$		$L_{z'}$
$P_L^\gamma \sin(2\phi_\gamma)$		H		G	$O_{x'}$		$O_{z'}$		$C_{z'}$		E		F		$-C_{x'}$	
$P_L^\gamma \cos(2\phi_\gamma)$	$-\Sigma$		$-P$			$-T$		$-L_{z'}$		$T_{z'}$		$-\sigma_0$		$L_{x'}$		$-T_{x'}$
circular P_c^γ		F		$-E$	$C_{x'}$		$C_{z'}$		$-O_{z'}$		G		$-H$		$O_{x'}$	

Full set of 16

status	CLAS run period	beam	target
complete	g1c, g11a	γ , $\vec{\gamma}_c$	LH_2
complete	g8	$\vec{\gamma}_L$	LH_2
complete	g9a - P^T_z	$\vec{\gamma}_L$, $\vec{\gamma}_c$	FROST - $C_4\vec{H}_9O\vec{H}$
complete	g9b - P^T_x	$\vec{\gamma}_L$, $\vec{\gamma}_c$	FROST - $C_4\vec{H}_9O\vec{H}$

⇔ PR C**73**(06); C**75**(07); C**81**(10)

FROST: frozen-spin target

- target: Ø 15mm x 50mm
- material: C_4H_9OH -butanol
- dilution factor: 10/74

- P(H) = 83%
- T_1(1/e relaxation time)
  = 115 d (+ pol)
  = 65 d (- pol)
- repolarize ~ once/week

<u>Polarization mechanism</u>:

- polarize electrons at 0.4 K and 5 Tesla
- e ➔ H transfer w μWaves
- drop temp to 30 mK to increase T_1

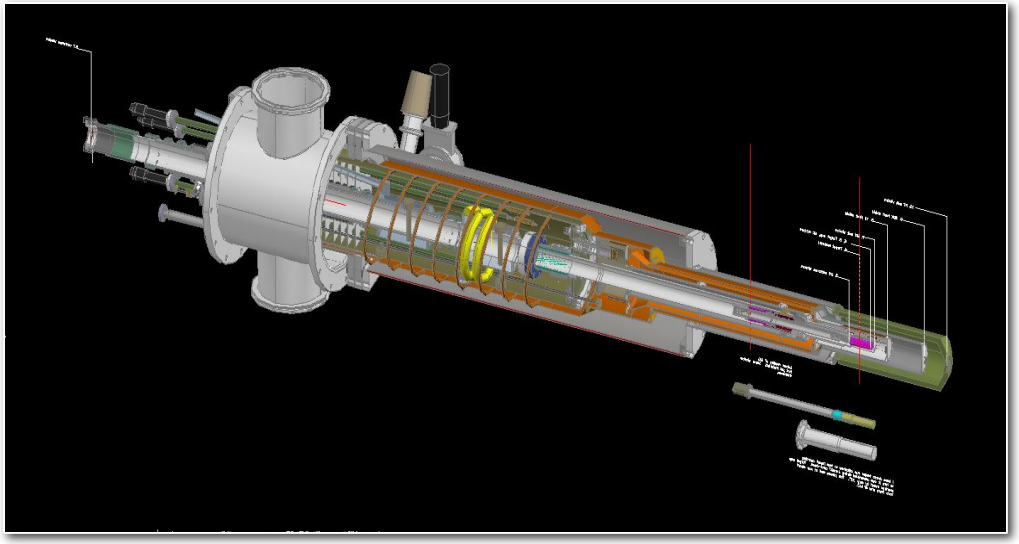

$K^+\Lambda$ observables:

χ^2 = 1.54 -to- 2.16

E_γ = 1421 (W = 1883) MeV

Published results:

- CLAS g1c: $d\sigma$, $C_{x'}$, $C_{z'}$
- CLAS g11a: $d\sigma$, P
- GRAAL: Σ, T, P, $O_{x'}$, $O_{z'}$

new PRELIMINARY data:
(C. Paterson, thesis – Glasgow'08)

- CLAS g8: Σ, T, P, $O_{x'}$, $O_{z'}$

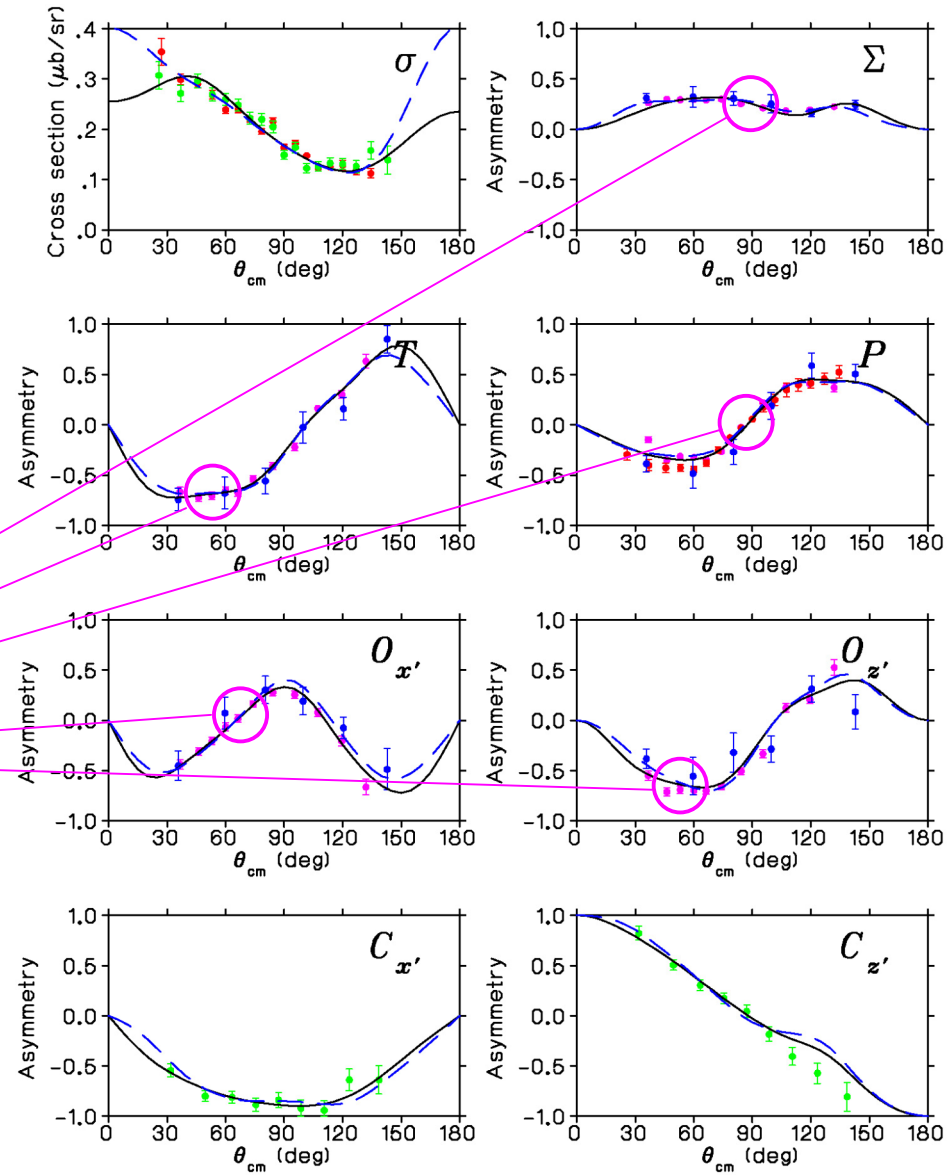

$K^+\Lambda$ observables:

χ^2 = 1.54 -to- 2.16
E_γ = 1421 (W = 1883) MeV

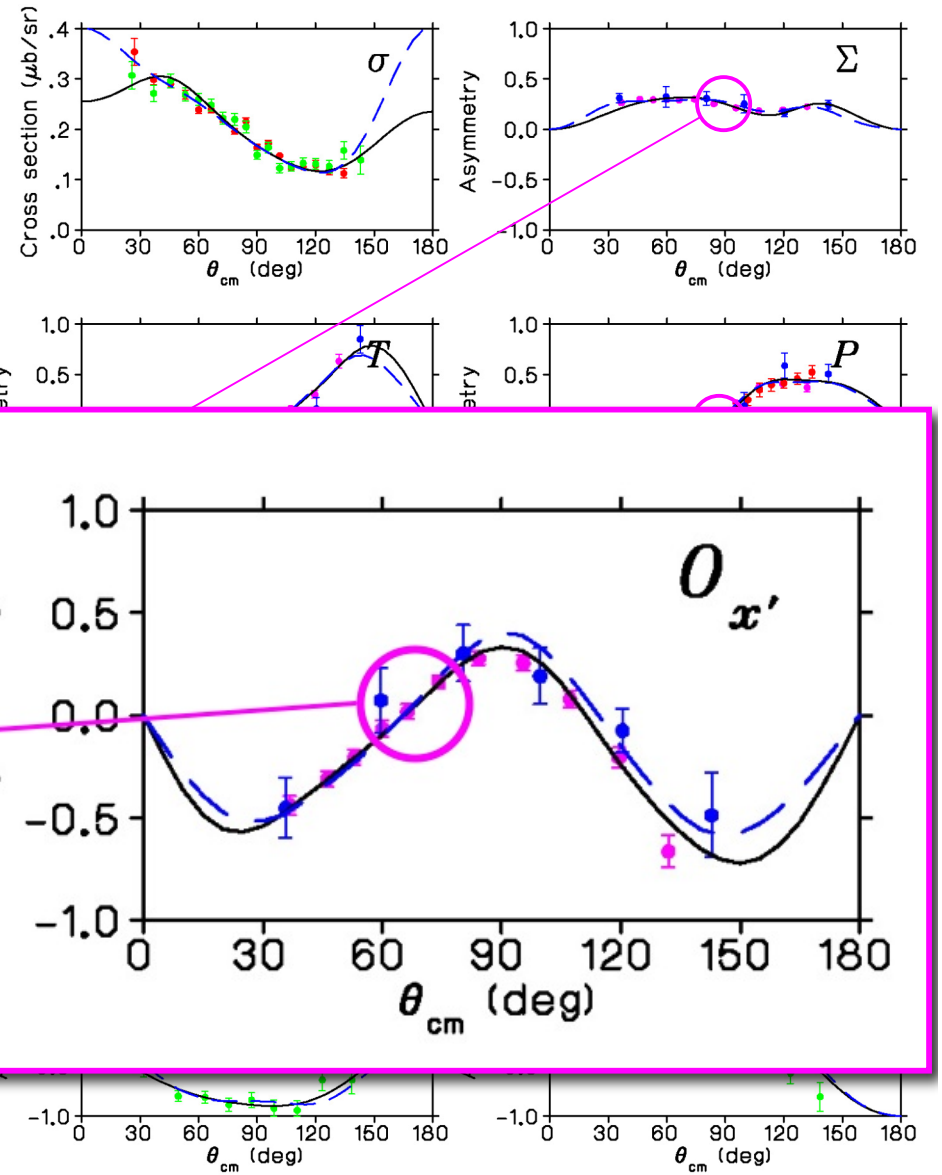

Published results:

- CLAS g1c: $d\sigma$, $C_{x'}$, $C_{z'}$
- CLAS g11a: $d\sigma$, P
- GRAAL: Σ, T, P, $O_{x'}$, $O_{z'}$

new PRELIMINARY data:
(C. Paterson, thesis – Glasgow'08)

- CLAS g8: Σ, T, P, $O_{x'}$, $O_{z'}$
  - very small statistical errors

Polarization observables in γn (p) $\rightarrow K^0\Lambda$ photo-production :

Photon beam		Target			Recoil			Target - Recoil								
					x'	y'	z'	x'	x'	x'	y'	y'	y'	z'	z'	z'
		x	y	z				x	y	z	x	y	z	x	y	z
unpolarized	σ_0		T			P		$T_{x'}$		$L_{x'}$		Σ		$T_{z'}$		$L_{z'}$
$P_L^\gamma \sin(2\phi_\gamma)$		H		G	$O_{x'}$		$O_{z'}$		$C_{z'}$		E		F		$-C_{x'}$	
$P_L^\gamma \cos(2\phi_\gamma)$	$-\Sigma$		$-P$			$-T$		$-L_{z'}$		$T_{z'}$		$-\sigma_0$		$L_{x'}$		$-T_{x'}$
circular P_c^γ		F		$-E$	$C_{x'}$		$C_{z'}$		$-O_{z'}$		G		$-H$		$O_{x'}$	

Full set of 16

status	CLAS run period	beam	target
complete	g13	$\vec{\gamma}_L$	LD_2
~ complete	g14	$\vec{\gamma}_L$, $\vec{\gamma}_c$	$H\vec{D}ice$

HDice: Frozen-spin Target

- target: ∅ 15 mm × 50 mm
- material: solid HD
- dilution factors: 1/2 for $\vec{p}$
  1/1 for $\vec{n}$

- P(H) = 60% or P(D) = 30%
- T_1 (1/e relaxation time)
  ~ years
- no repolarization needed

Polarization mechanism:

- polarize impurities (10^{-3}) of H_2 and D_2 at 0.010 K and 15 Tesla
- spin exchange w HD
  $\vec{H}_2 \Rightarrow \vec{H}\vec{D} \Leftarrow \vec{D}_2$
- wait for H_2 and D_2 to decay to inert ground st (~ 3 months)

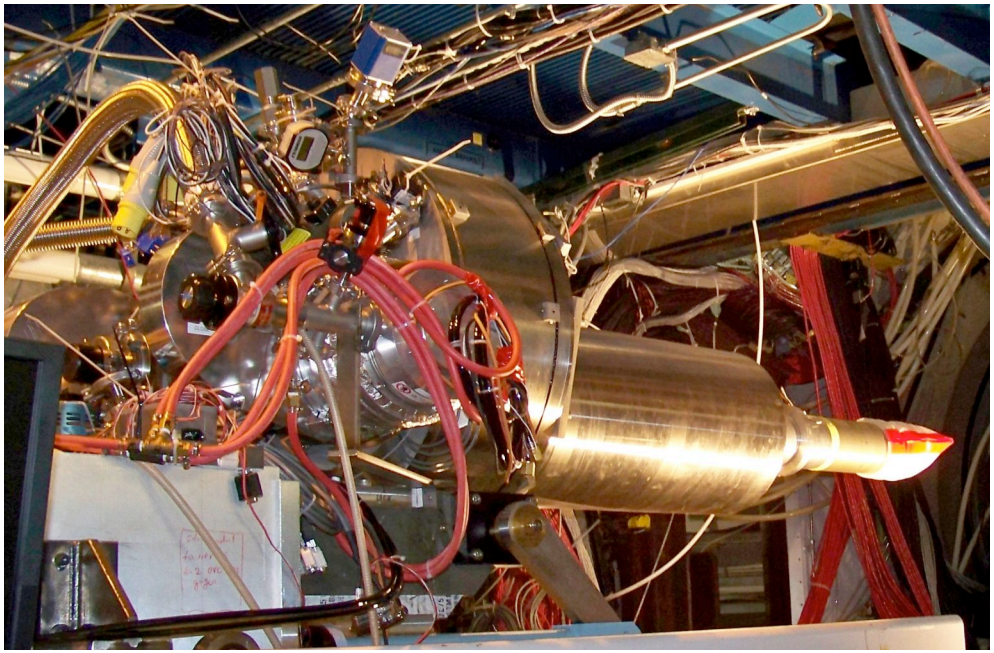

External Magnetic field rapidly aligns Ortho-H_2 and Para-D_2 then spins exchange with H and D in HD

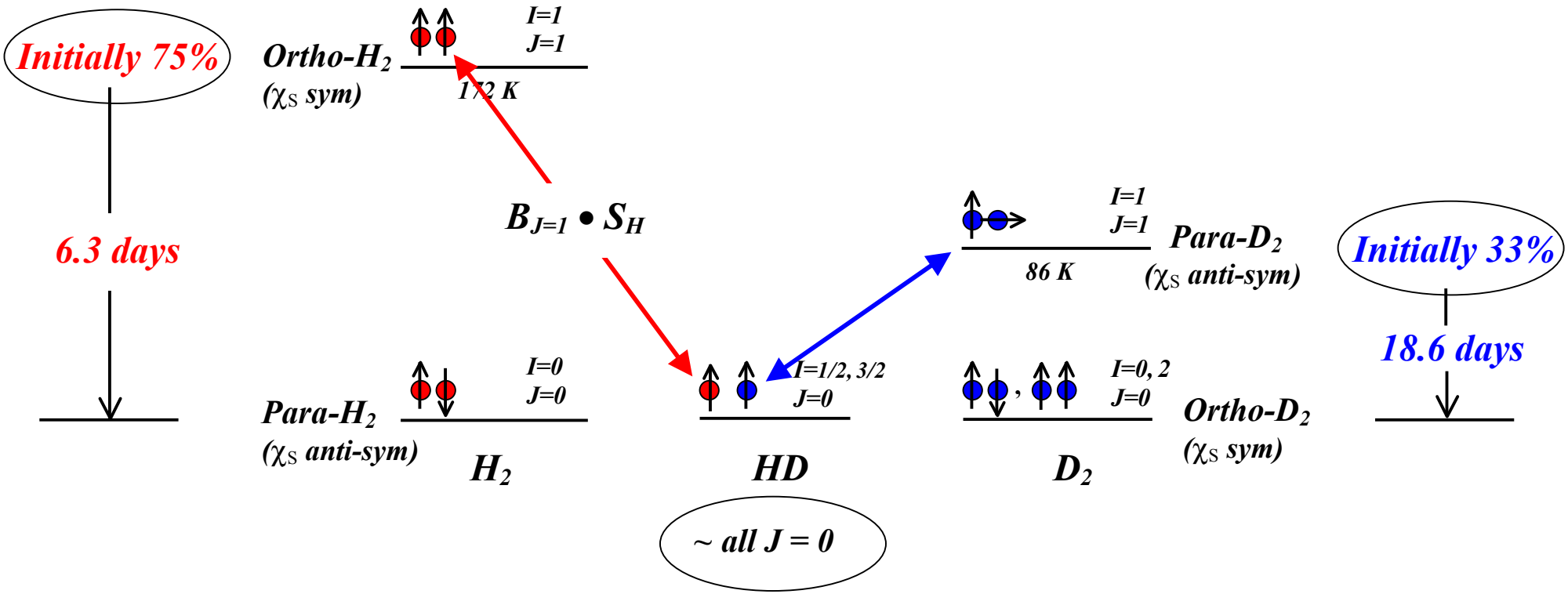

- *relaxation switch – A. Honig, Phys. Rev. Lett.* ***19*** *(1967).*

$\vec{H}\vec{D}$ice polarize/freeze spins/run exp sequence

HDice Target Lab

- condense HD gas → liquid → solid at 16°K
- calibrate pol-NMR at 2°K and 0.2 tesla
- transfer to dilution refrigerator & polarize at 15 Tesla and 10 mK
- hold at high-field and low-temp for >3 months
- transfer to 5 Tesla/1.6°K Storage Cryostat

⇒

transfers are the trickest part

Hall-B

- move to Hall B (~ 1 Km)
- transfer to In-Beam Cryostat (IBC)
- move spins $\vec{H} \Leftrightarrow \vec{D}$ w rf as needed
- roll IBC into CLAS
- run the exp

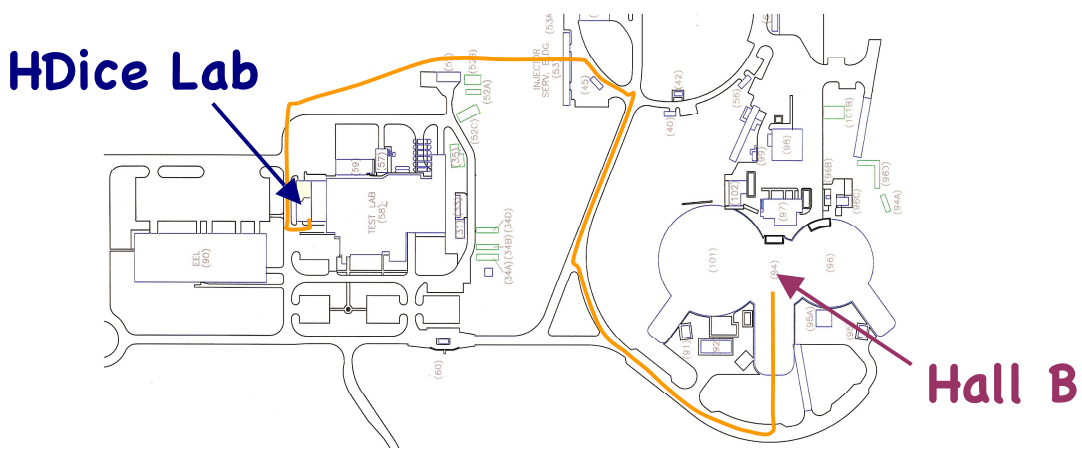

High field/low temperature TE limit :

- 15T/10mK ⇒ P(H) = 90% ; P(D) = 30%

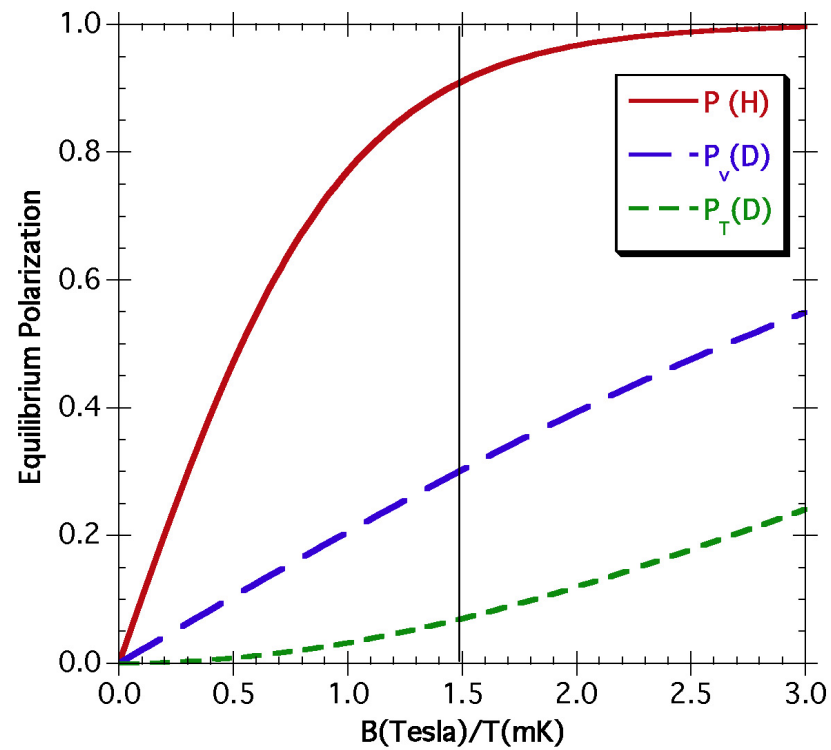

But:

- time to TE = relaxation time ∝ B/T

  ⇒ very long at High B/Low T

  ⇔ keeps getting longer as o-H_2 & p-D_2 J=1 impurity states decay

  ⇔ would need to increase J=1 states to provide time to reach TE

- heat from J=1 o-H_2 & p-D_2 decays must be carried away in order to reach TE

  - heat conducted through HD via phonons
  - limited by scattering from J=1 rotational states in o-H_2 & p-D_2 impurities

  ⇔ HD can't reach low temperature until J=1 impurities decay

⇒ these two effect fight each other and reach a balance that is almost independent of initial o-H_2 & p-D_2 concentrations:

⇒ **P(H) ~ 60 ±5% ; P(D) ~ 15 ±7%**

D polarization during g14/E06-101

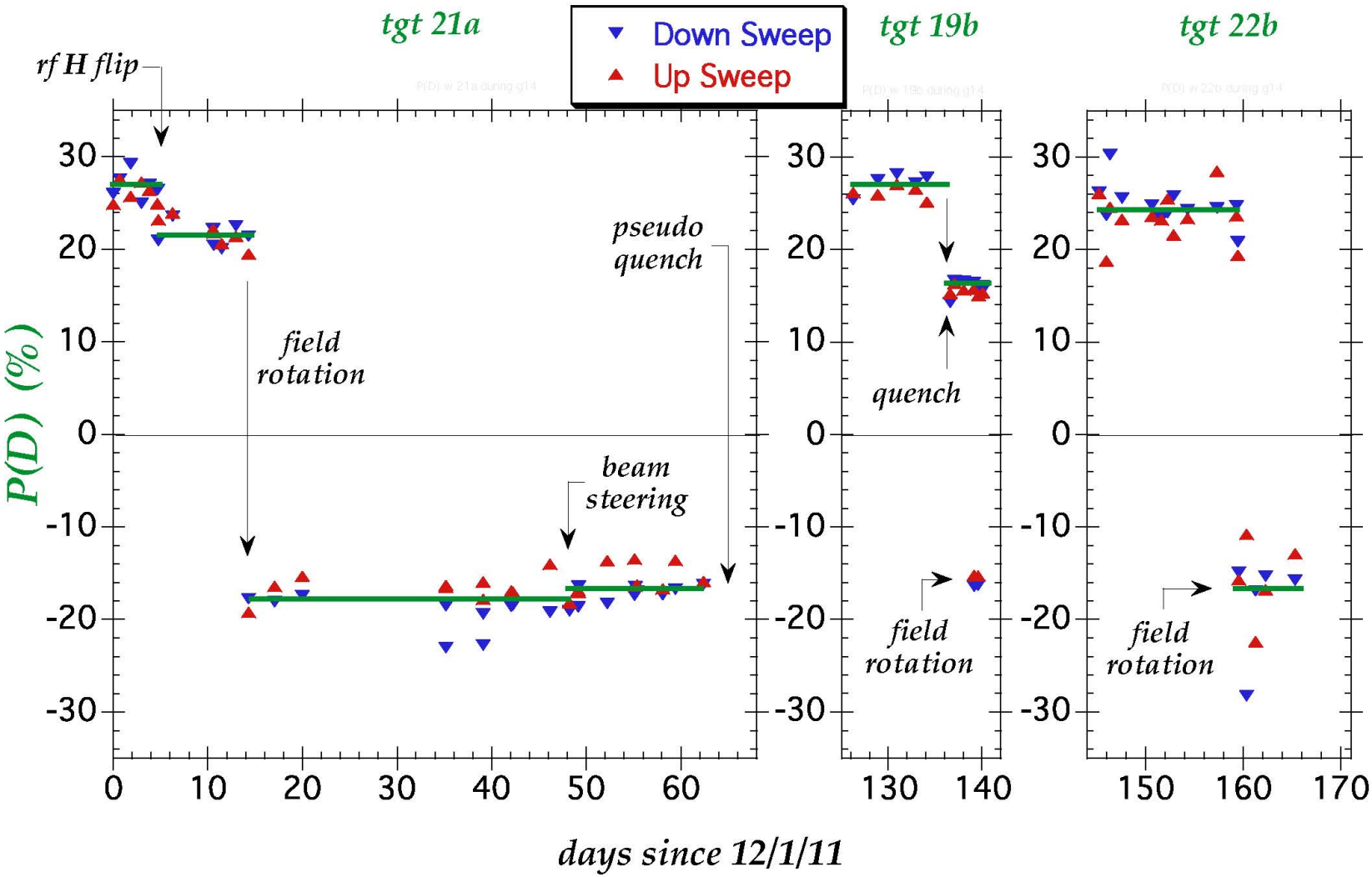

- Polarization × HDice dilution ~ similar to FROST polarization × dilution
- HDice experiments able to run at 10 times higher fluxes (due to low Z)

1st look at neutron data from g14 / $\vec{H}$Dice (concluded May 18th/12)

- $\vec{\gamma}\,\vec{n}\,(p) \rightarrow \pi^{-}\,p\,(p)$
- E beam-target helicity asymmetry from a few % of the g14 data:

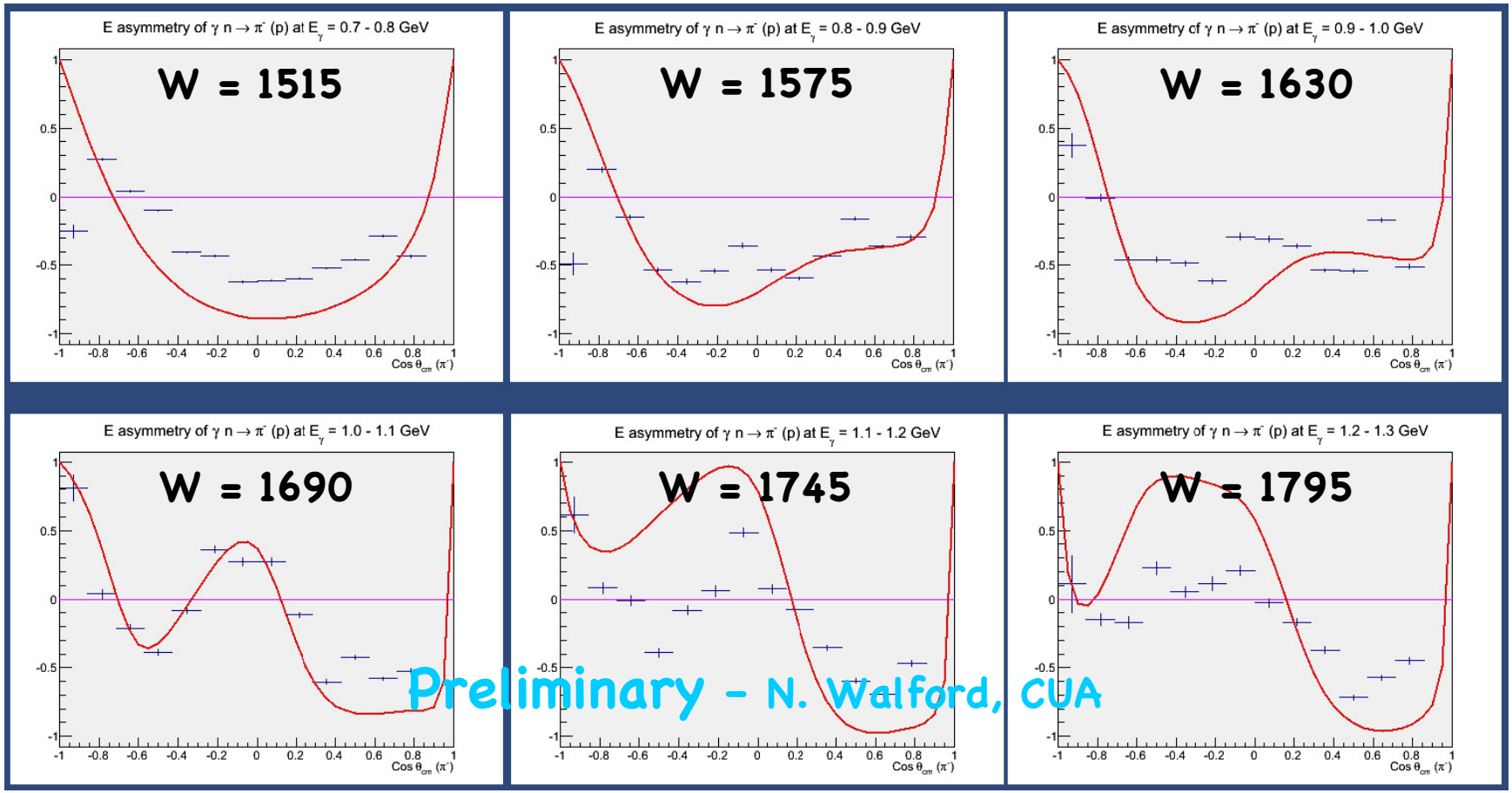

— SAID extrapolations from proton data

$\gamma\, p \rightarrow K^{+}\Lambda$ data in the pipe-line

- **published CLAS data:**

Experiment	*Observable*	*Eγ range / W range*	*ΔEγ / ΔW binning*	*Publications*
CLAS-**g1c**	$d\sigma$, P, $C_{x'}$, $C_{z'}$	**1032 – 2741** 1679 – 2454	**100**	PR C**73**,35202(06) PR C**75**,35205(07)
CLAS-**g11a**	$d\sigma$, P	**938 - 3813** 1625 - 2835	10	PR C**81**,25201(10)

- **new preliminary (theses) data near final stages of analyses:**

Experiment	*Observable*	*Eγ range / W range*	*ΔEγ / ΔW binning*	*CLAS thesis*
CLAS-**g8**	Σ, T, P, $O_{x'}$, $O_{z'}$	**1025 – 2075** 1675 – 2185	**50**	C. Paterson (*Glasgow'08*)
CLAS-**g9a**	Σ, G	**1010 – 2100** 1720 – 2195	100	S. Fegan (*Glasgow'11*)
CLAS-**g9a**	E, $L_{x'}$, $L_{z'}$	**1050 – 2275** 1690 – 2270	**100**	L. Casey (*Catholic U A'11*)
CLAS-**g9a, g9b**, **g14**	***many more in the queue***			

Unraveling the Excitation Spectrum of the Nucleon
- the N* Program at Jefferson Lab

A.M. Sandorfi
Thomas Jefferson National Accelerator Facility, Virginia USA

- current quarks, constituent quarks & real world "dressings"
- the problem with the N* spectrum
  … and the hyperon solution – measurements of *everything*
- the CLAS g9/FROST and g14/HDice experiments
- *eg.* $\gamma p \rightarrow K^+\Lambda$ from what we know now,
  and what we can expect …

Analyses of $\gamma\, p \rightarrow K^+\Lambda$

- **published CLAS data:**

Experiment	*Observable*	*Eγ range / W range*	*ΔEγ / ΔW binning*	*Publications*
CLAS-**g1c**	$d\sigma$, P, $C_{x'}$, $C_{z'}$	**1032 – 2741** 1679 – 2454	**100**	PR C**73**,35202(06) PR C**75**,35205(07)
CLAS-**g11a**	$d\sigma$, P	**938 - 3813** 1625 - 2835	10	PR C**81**,25201(10)

- **Bonn-Gatchina PWA,** [Anisovich *et al*, Eur Phys J A48 (12) 14]
  including CLAS and CB-ELSA data on $\gamma\, p \rightarrow K^+\Lambda$, $K^+\Sigma^0$, $K^0\Sigma^+$

⇒ **"new" N*** — **BnGa STAR ratings**

	$K\Lambda$	$K\Sigma$
N(1880)1/2⁺	☆☆	☆
N(1895)1/2⁻	☆☆	☆
N(1875)3/2⁻	☆☆☆	☆☆
N(2150)3/2⁻	☆☆	
N(2060)5/2⁻		☆☆

⇒ **intriguing, although STAR-confidence levels probably optimistic due to the presence of ambiguous multiple solutions**

Multipole Analysis of $\gamma\, p \rightarrow K^+\Lambda$ with 8 published observables

- **published data**

Data group	*Experiment*	*Observable*	*Eγ range / W range*	*ΔEγ / ΔW binning*	*Systematic Scale error*
1	CLAS-g11a	$d\sigma$	**938 – 3814** 1625 – 2835	10	±8% (*Eγ dependent*)
2	CLAS-g11a	P	**938 – 3814** 1625 – 2835	10	±0.05
3	CLAS-g1c	$C_{x'}$, $C_{z'}$	**1032 – 2741** 1679 – 2454	**101**	±0.03
4	CLAS-g1c	$d\sigma$	**944 – 2950** 1628 – 2533	25	±8% (*Eγ dependent*)
5	GRAAL	$O_{x'}$, $O_{z'}$	**980 – 1466** 1649 – 1906	50	±4%
6	GRAAL	P	**980 – 1466** 1649 – 1906	50	±3%
7	GRAAL	Σ	**980 – 1466** 1649 – 1906	50	±2%
8	GRAAL	T	**980 – 1466** 1649 – 1906	50	±5%

- **limited common energy range: E_γ = [1027, 1421]; W = {1676, 1883}**

Multipole fitting procedure –cont':

- fix L = 4-8 multipoles to their (real) Born values
- Monte Carlo sampling of real and imaginary parts of L=0-3 multipoles – up to 10^7 per energy
- gradient minimization (with MINUIT) whenever χ^2 within 10^4 of current best
- choose a reference point for the overall phase – eg. $\delta(E_{0+}) = 0$

Results for the combined g1c, g11a and GRAAL data sets:

$\Rightarrow$ $\exists$ bands of solutions with tightly clustered χ^2 : [SHKL, J Phys G38(11)053001]

E_γ / W (MeV)	Best χ^2/pt	Largest χ^2/pt
1027 / 1676	0.49	0.54
1122 / 1728	0.59	0.62
1222 / 1781	0.52	0.62
1321 / 1833	0.74	0.92
1421 / 1883	0.97	1.15

$K^+\Lambda$ multipoles: —— Best χ^2 - - - Largest χ^2

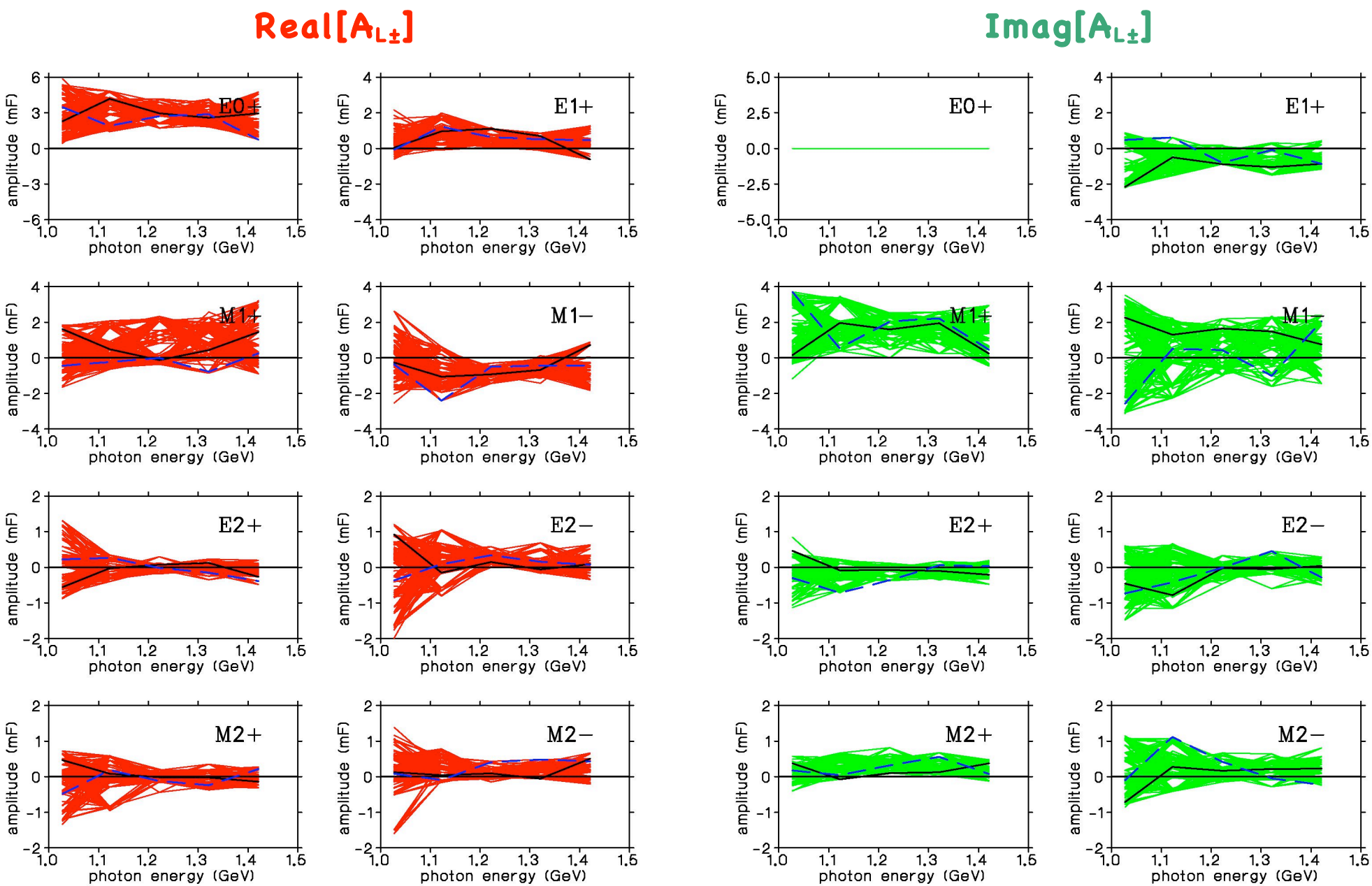

$K^+\Lambda$ observables:

—— Best χ^2 — — — Largest χ^2

exp indistinguishable

E_γ = 1122 (W = 1728) MeV

E_γ = 1421 (W = 1883) MeV

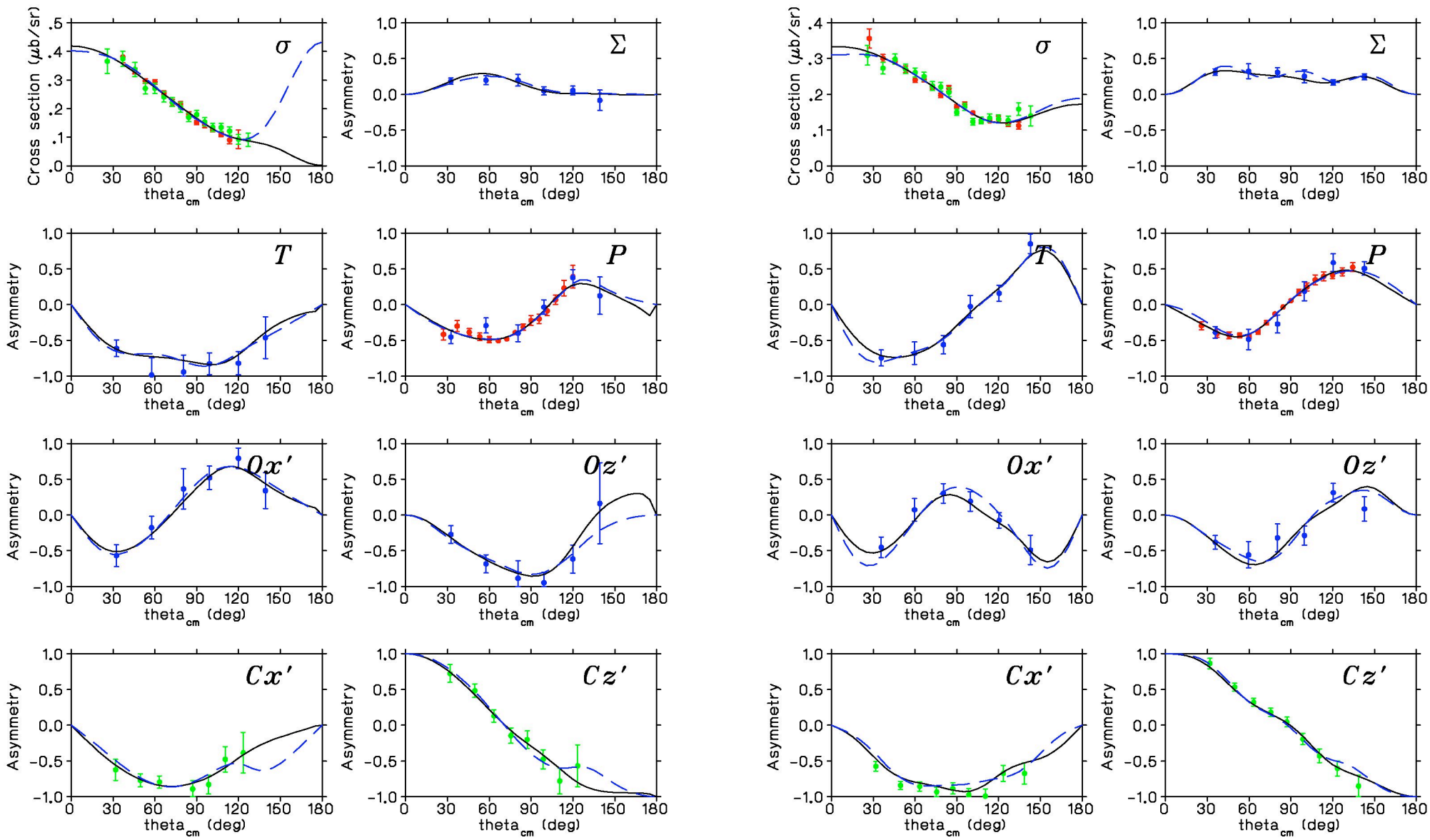

The χ^2 surface - valley or mine-field ?

- construct a hybrid amplitude from any two solutions; track χ^2 between them.

$$A_h(x) = A_1\left(1 - \frac{x}{100}\right) + A_2\left(\frac{x}{100}\right) ,$$

$$x \in [0, 100]$$

- if $\chi^2(x)$ is smooth,
  - multiple solutions
    $\Leftrightarrow$ ill-defined shallow χ^2 minimum

- if $\chi^2(x)$ shows peaks,
  - multiple solutions
    $\Leftrightarrow$ real multiple local minima

The χ^2 surface – valley or mine-field ?

- construct a hybrid amplitude from any two solutions; track χ^2 between them.

$$A_h(x) = A_1\left(1-\frac{x}{100}\right)+A_2\left(\frac{x}{100}\right),$$

$$x \in [0,\ 100]$$

- there is always a peak between any two solutions !

$\Rightarrow$ the solution bands are clusters of many degenerate local minima

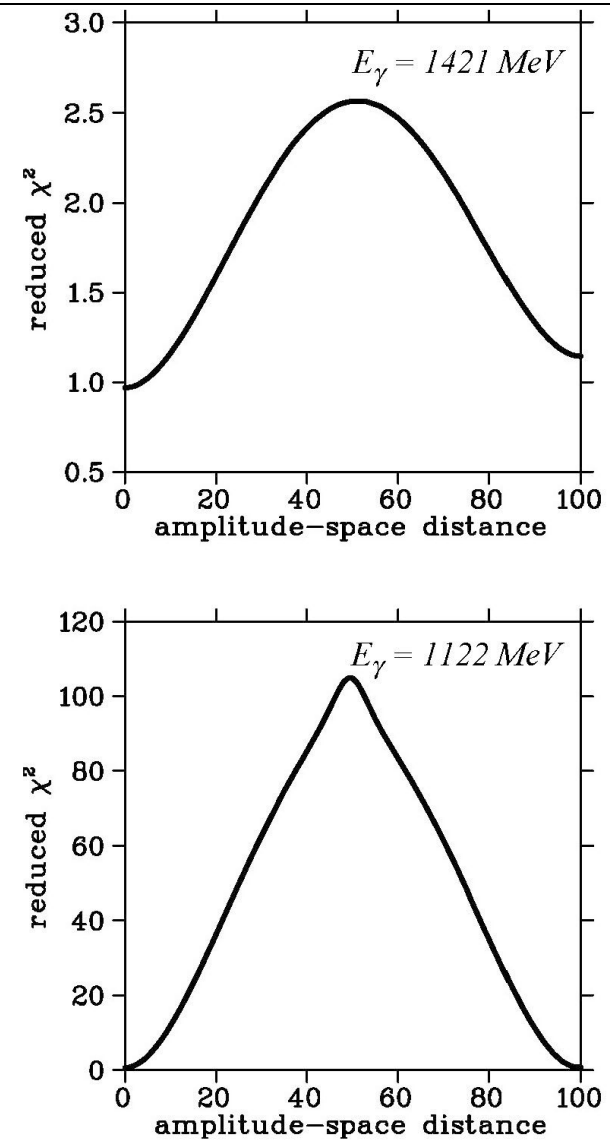

χ^2 between Best and Worst solutions

The potential of *complete* experiments - studies with mock data

- generate mock data, using BoGa multipoles, at energies and angles of the CLAS data sets

- vary positions of mock points by sampling Gaussians of widths that reflect different levels of uncertainty

- creating pseudo (mock) data:
  - curve predicted from assumed multipoles
  - mock data point placed on curve at expected kinematic settings
  - randomly pick value for each point within a Gaussian of width equal to expected errors

eg.

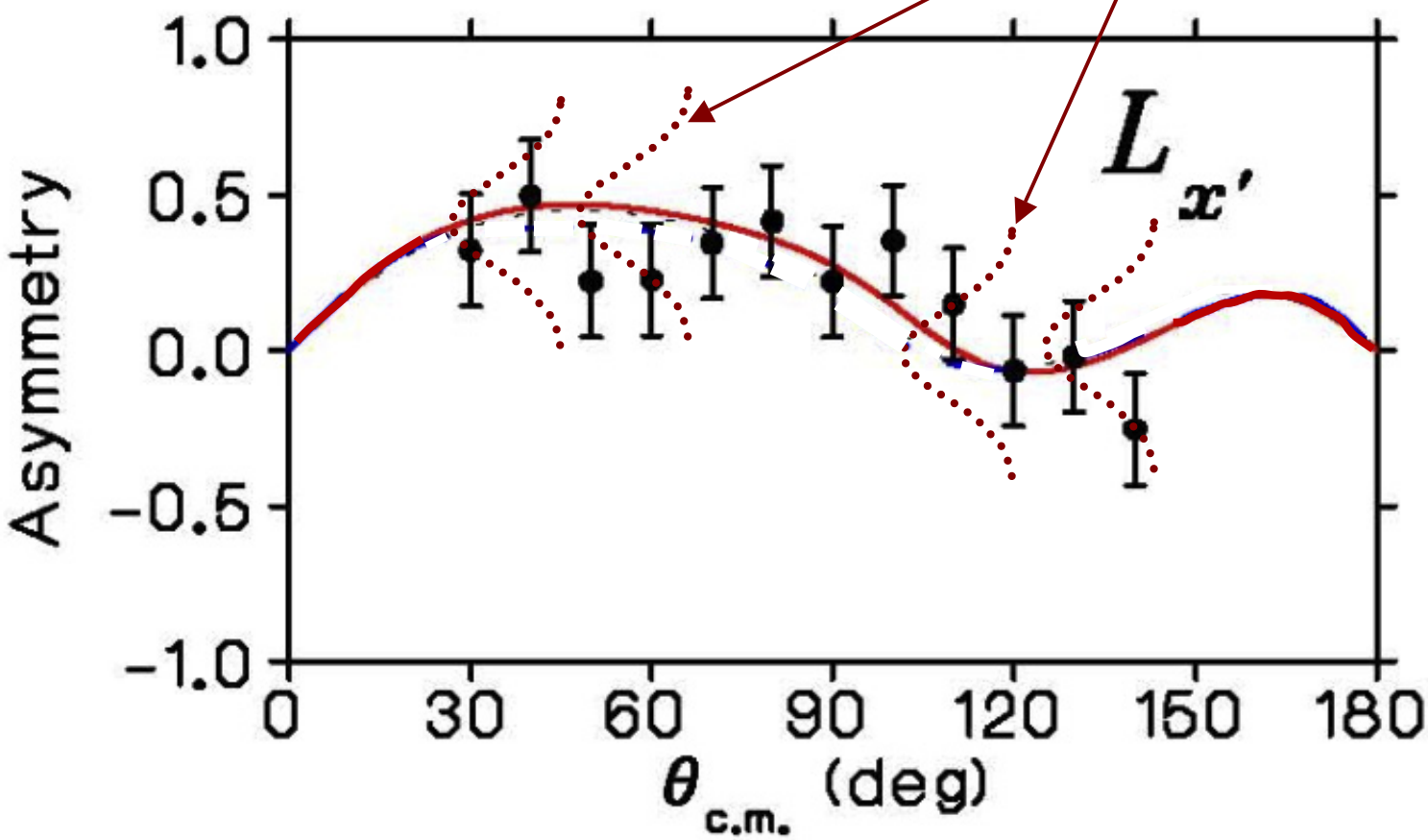

Simulated $K^+\Lambda$ CLAS results:

- points generated from BoGa multipoles, W = 1900
- errors from CLAS runs g1c, g8, g11a, and estimated errors for g9-FROST

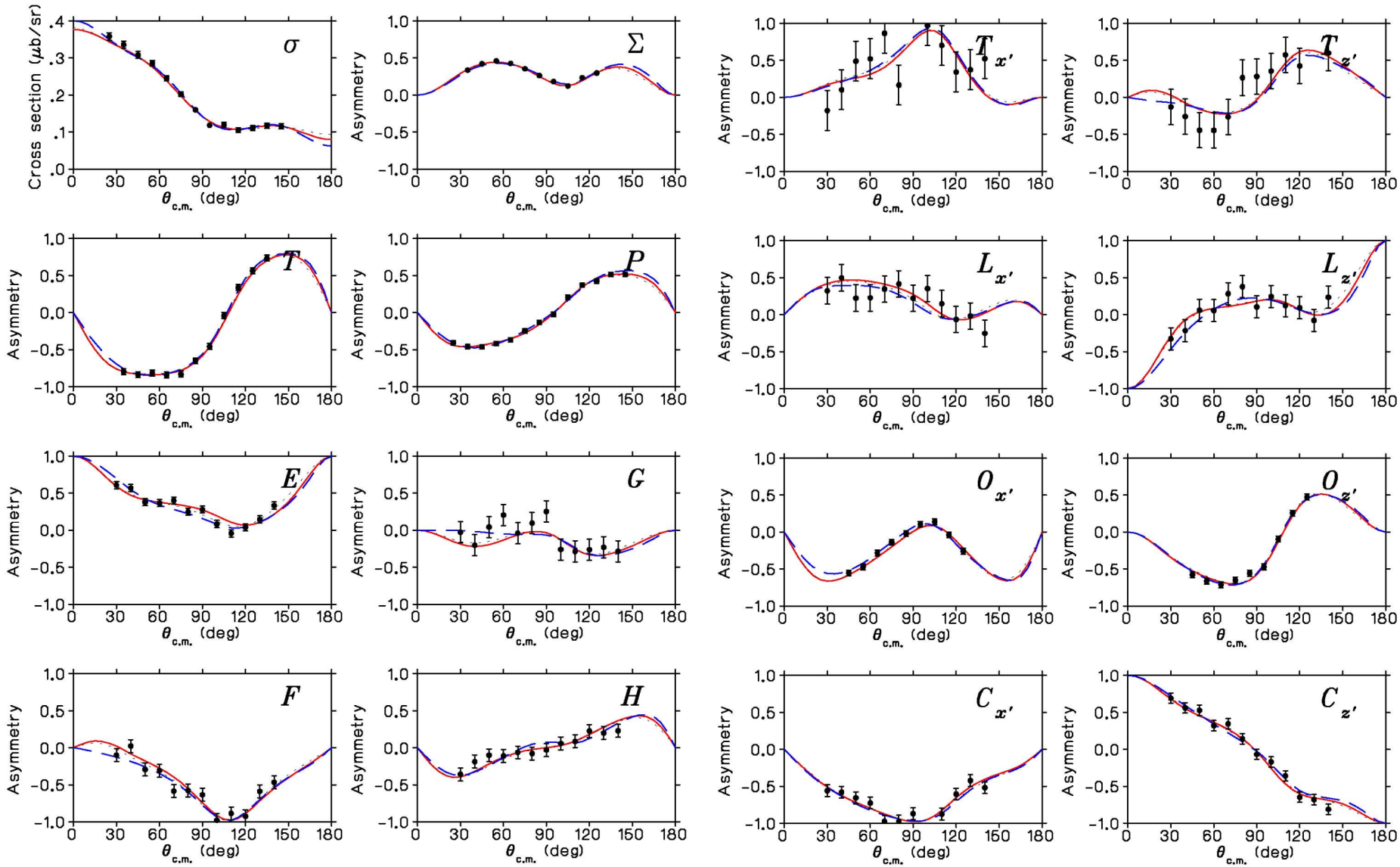

The potential of *complete* experiments - studies with mock data

- generate mock data, using BoGa multipoles, at energies and angles of the CLAS data sets

- vary positions of mock points by sampling Gaussians of widths that reflect different levels of uncertainty

- fit mock data with the assumed uncertainties by varying multipoles, L=0-3
  - Monte Carlo sampling, with gradient minimization
  - phase constrained by a real E_{0+}

Expected accuracy of $K^+\Lambda$ multipole determination from CLAS results

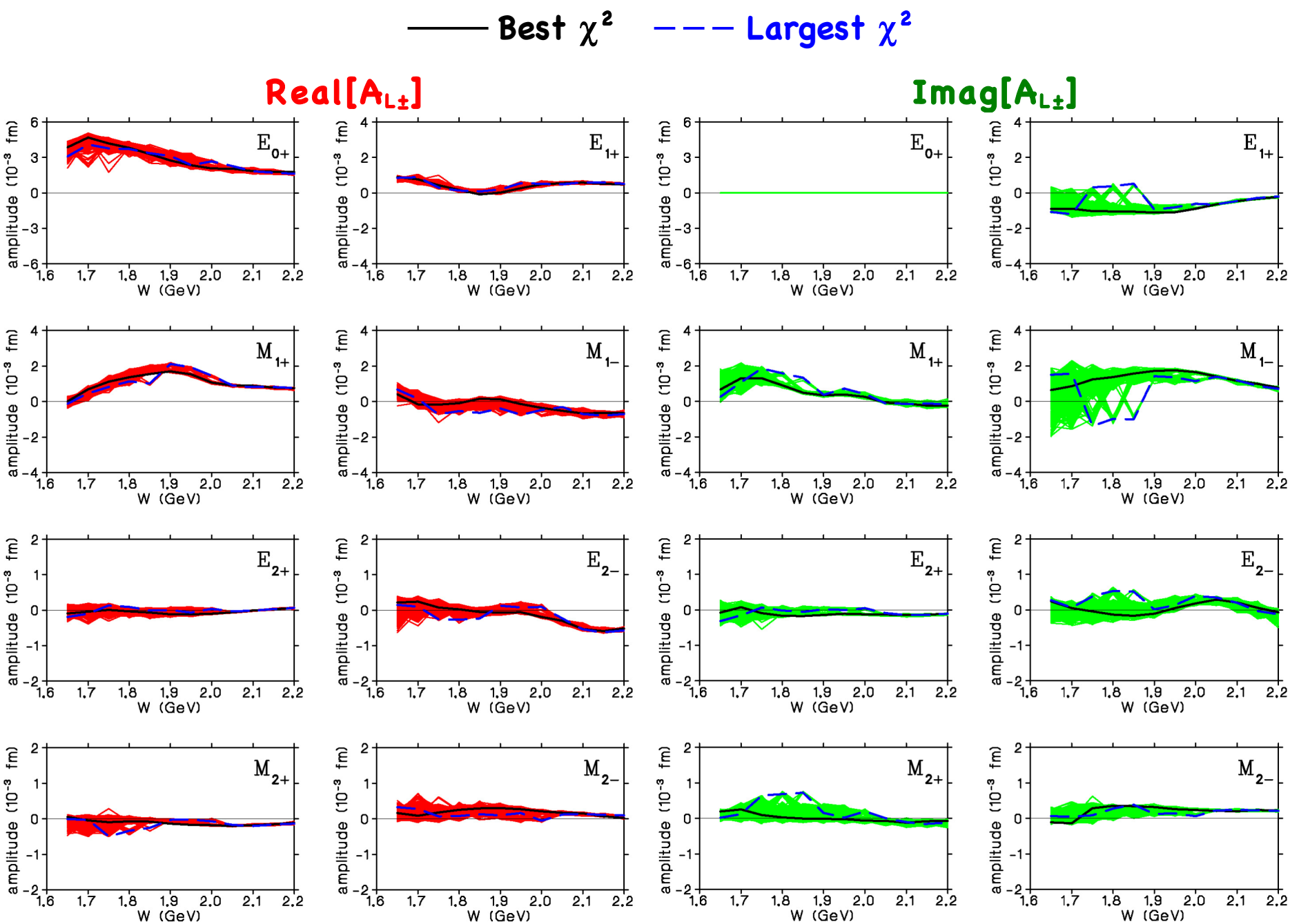

Simulated CLAS16 K+L bands –fig 19,20

- ideal single isolated resonance

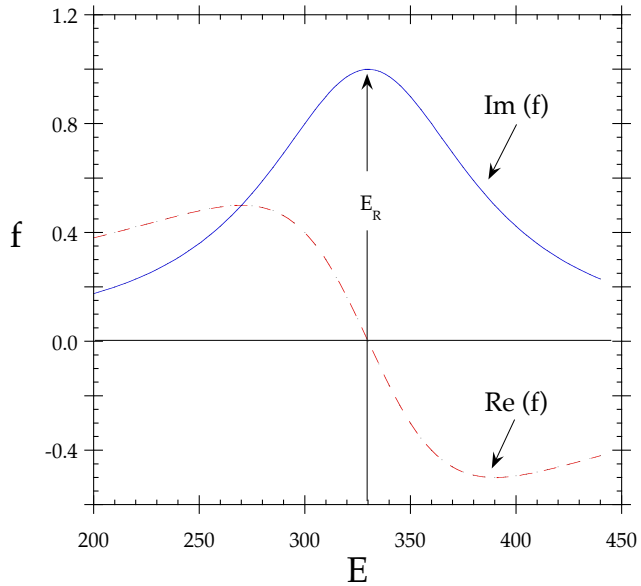

- weak state in EBAC model of KΛ production

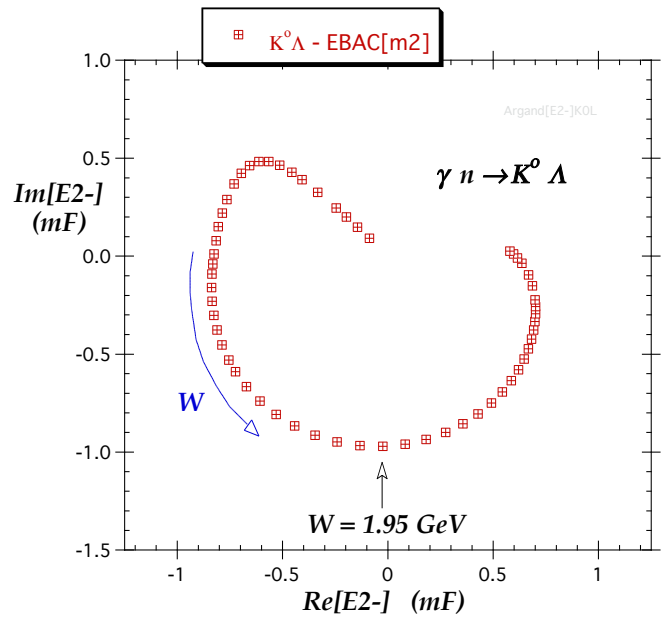

Argand plots:

- counter-clockwise rotating amplitude
  - characteristic resonance behavior

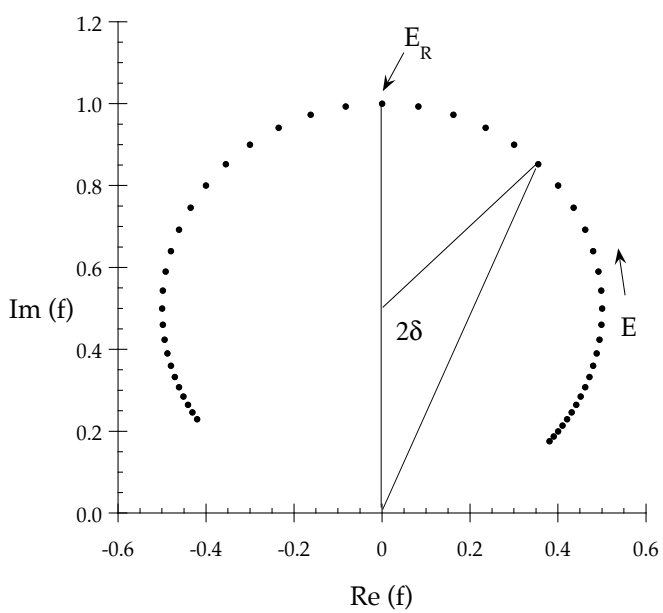

- fits to mock E06-101 data
with expected statistics and kinematic coverage

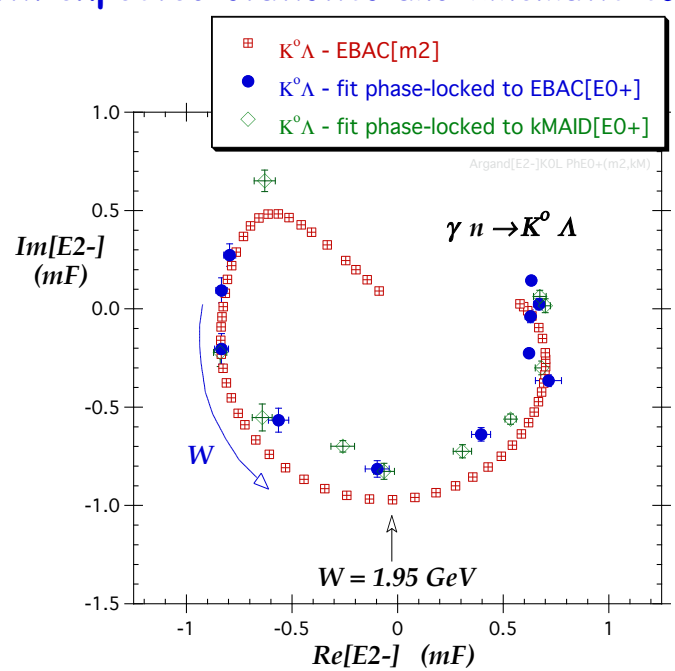

Summary

- $K\Lambda$ and $K\Sigma^+$ channels provide opportunities to accumulate all 16 spin observables in photo-production

- $\exists$ large sets of new single, double and triple polarization data on the proton and neutron that are under analysis. The prospects for determining the amplitude in at least a few photo-production channels are very good.

- expect many multipoles to be well determined, providing a new window to the N* spectrum

A few caveats:

- given realistic errors, number of observables needed to determine an amplitude with reasonable uncertainty is much more than the "8" required for a "mathematical solution"

- nonetheless, with measurements of all 16 observables, data with even modest errors will have a big impact !